

Electromagnetic Form Factors of the SU(3) Octet Baryons in the semibosonized SU(3) Nambu-Jona-Lasinio Model

Hyun-Chul Kim ^{*}, Andree Blotz [†], Maxim Polyakov [‡] and Klaus Goeke [§]

Institute for Theoretical Physics II,

P.O. Box 102148, Ruhr-University Bochum,

D-44780 Bochum, Germany

(July 10, 2018)

Abstract

The electromagnetic form factors of the SU(3) octet baryons are investigated in the semibosonized SU(3) Nambu–Jona-Lasinio model (chiral quark-soliton model). The rotational $1/N_c$ and strange quark mass corrections in linear order are taken into account. The electromagnetic charge radii of the nucleon and magnetic moments are also evaluated. It turns out that the model is in

^{*}E-mail address: kim@hadron.tp2.ruhr-uni-bochum.de

[†]Present address: Department of Physics, State University of New York, Stony Brook, 11794, U.S.A.

[‡]On leave of absence from Petersburg Nuclear Physics Institute, Gatchina, St. Petersburg 188350, Russia

[§]E-mail address: goeke@hadron.tp2.ruhr-uni-bochum.de

a remarkable good agreement with the experimental data.

12.40.-y, 13.40.Em, 13.40.Gp, 14.20.Dh, 14.20.Jn

I. INTRODUCTION

In spite of the belief that Quantum Chromodynamics (QCD) is the fundamental underlying theory of the strong interaction, low energy phenomena such as static properties of hadrons defy solutions based on QCD. The pertinacity of QCD in the low energy region have led to efforts to construct an effective theory for the strong interaction. In pursuit of this aim, the chiral quark soliton model—also known as the semibosonized Nambu-Jona-Lasinio(NJL) model—emerged as a successful effective theory to describe the low energy phenomena without loss of important properties of QCD such as chiral symmetry and its spontaneous breaking.

Originally, the idea of finding the soliton in a model with quarks coupled to pions was realized by Kahana, Ripka and Soni [1] and Banerjee and Birse [2]. The bound states of the valence quarks were well explored in the model while it suffered from the vacuum instability [3]. This problem of the vacuum instability was solved by Diakonov and Petrov [4]. Having investigated the instanton picture of the QCD vacuum in the low-momenta limit in Ref. [4], they have shown that the low-momenta theory is equivalent to the quark-soliton model free from the vacuum instability. The model was further elaborated in Ref. [5] so that it could predict the static properties of the nucleon in the gradient approximation.

The baryon in this model is regarded as N_c valence quarks coupled to the polarized Dirac sea bound by a non-trivial chiral field configuration in the Hartree approximation [5–8]. The identification of the baryon quantum numbers is acquired by the semi-classical quantization [5,9] (in nuclear physics called the cranking method [10]) which is performed by integrating over the zero-mode fluctuations of the pion field around the saddle point. It makes the baryon carry proper quantum numbers like spins and isospins. In SU(2), the model enables us to describe quantitatively a great deal of static properties of the nucleon such as N - Δ splitting [8,11], axial constants [8,12,13], electromagnetic form factors [14,15], and to some extent also magnetic moments [8,15].

Although the SU(2) version of the model was quite successful to explain many static

properties of the nucleon, it is necessary to extend the model from SU(2) to SU(3) so that it can be possible to examine the same properties of hyperons and moreover to investigate the effects of hidden strangeness on the nucleon which are in particular manifested in the πN sigma term [16,17], the iso-splitting of the baryonic masses [18] and strange form factors [19]. Blotz *et al.* [22,23] and Weigel *et al.* [24] have carried out the extension of the model from SU(2) to SU(3). Starting from the semibosonized NJL-type lagrangian, they have shown that the model describes hyperon spectra successfully. The extended SU(3) model is distinguished from the SU(2) NJL in two ways: Firstly, the mixed terms of the pure SU(2) part and the strange vacuum part are induced by the trivial embedding of the SU(2) soliton into SU(3). Secondly, since the mass of the strange is not negligible, one has to take into account the mass term in the effective action explicitly. The mass corrections are treated perturbatively in linear order. It was shown that the perturbative treatment of the m_s in the NJL model describes the octet-decuplet mass splitting [22,23] very well and plays an essential role in the mass splitting of hyperons. These two differences determine the characteristic of the SU(3) NJL model.

Refs. [22,24] indicate that the SU(3) NJL provides a more refined structure of the collective hamiltonian than the pseudoscalar Skyrme model. A comparable structure can be obtained in the Skyrme model only by introducing explicit vector mesons. However, it is inevitable to import large numbers of parameters into the Skyrme model with vector meson, while the parameters in the NJL model can be fixed completely by adjusting mesonic masses and decay constants (f_π , f_K). The only free parameter we have is the constituent quark mass arising as a result of the spontaneously broken chiral symmetry. This parameter is fixed by adjusting the mass splitting [23] properly.

It is of great importance that $1/N_c$ rotational corrections are taken into account. Starting from the path integral formalism, when we integrate over zero modes fluctuations around the saddle point, a time ordered product of collective operators appears. The $1/N_c$ contribution survives due to the noncommutivity of the collective operators [12]. It was examined in detail in ref. [13] by calculating the axial vector constants g_A and isovector magnetic moments in

SU(2). In the same spirit, the SU(3) model was applied to obtain the axial constants $g_A^{(3)}$, $g_A^{(8)}$, and $g_A^{(0)}$ [20,21,25]. It predicted the experimental data within about 10%.

In recent papers, we have proceeded to evaluate the magnetic moments [28]. The magnetic moments of the SU(3) octet baryons predicted by the present model are in a remarkable agreement with the experiments.

Now, we are in a position to study the electromagnetic form factors and other form factors such as strange form factors. It is important to investigate the form factors in our model, since it allows us to take a step forward in studying dynamics. Hence, as a first phase, we will consider the electromagnetic form factors. It is of great significance to know them in the SU(3) NJL in that not only they provide us with the electromagnetic informations but also they allow us to proceed to explore the techniques for the form factors of the neutral(Z^0) currents and charged weak(W^\pm) currents.

The outline of the paper is as follows. In the next section, we develop the general formalism for the electromagnetic form factors in the SU(3) NJL. In section 3, we discuss the electric form factors with related quantities such as electric charge radii. In section 4, we continue to study the magnetic form factors of the SU(3) octet baryons. In section 5, we summarize the work and draw conclusions.

II. THE GENERAL FORMALISM

In this section, we present the general formalism for the electromagnetic form factors of the SU(3) octet baryons in the NJL.

The SU(3) NJL is characterized by a partition function in Euclidean space given by the functional integral over pseudoscalar meson and quark fields:

$$\begin{aligned} \mathcal{Z} &= \int \mathcal{D}\Psi \mathcal{D}\Psi^\dagger \mathcal{D}\pi^a \exp(-S_{NJL}) \\ &= \int \mathcal{D}\Psi \mathcal{D}\Psi^\dagger \mathcal{D}\pi^a \exp\left(-\int d^4x \Psi^\dagger iD\Psi\right), \end{aligned} \quad (1)$$

where D denotes the Dirac differential operator

$$iD = \beta(-i\not{\partial} + \hat{m} + MU) \quad (2)$$

with the pseudoscalar chiral field

$$U = \exp i\pi^a \lambda^a \gamma_5. \quad (3)$$

\hat{m} is the matrix of the current quark mass given by

$$\hat{m} = \text{diag}(m_u, m_d, m_s) = m_0 \mathbf{1} + m_8 \lambda_8. \quad (4)$$

λ^a represent the usual Gell-Mann matrices normalized as $\text{tr}(\lambda^a \lambda^b) = 2\delta^{ab}$. Here, we assume isospin symmetry, *i.e.* $m_u = m_d$. M shows the dynamical quark mass arising from the spontaneous chiral symmetry breaking, which is in general momentum-dependent [4]. For the sake of convenience we shall look upon M as a constant and introduce the ultra-violet cut-off via the proper time regularization which preserves gauge and chiral invariance [29].

The m_0 and m_8 in eq. (4) are respectively defined by

$$m_0 = \frac{m_u + m_d + m_s}{3}, \quad m_8 = \frac{m_u + m_d - 2m_s}{2\sqrt{3}}. \quad (5)$$

The operator iD is expressed in Euclidean space in terms of the Euclidean time derivative ∂_τ and the Dirac one-particle hamiltonian $H(U)$

$$iD = \partial_\tau + H(U) + \beta\hat{m} - \beta\bar{m}\mathbf{1} \quad (6)$$

with

$$H(U) = \frac{\vec{\alpha} \cdot \nabla}{i} + \beta MU + \beta\bar{m}\mathbf{1}. \quad (7)$$

β and $\vec{\alpha}$ are the well-known Dirac hermitian matrices [30]. The \bar{m} is defined by $(m_u + m_d)/2 = m_u = m_d$. We want to emphasize that the NJL model is a low-energy effective model of QCD. Hence, the action of this model can have, in principle, corrections from higher orders such as a term $\sim m^2 \Psi^\dagger \Psi$ for example. However, the coefficient in front of such a term is not known ¹ theoretically. Therefore, it is meaningless to go beyond the linear

¹The coefficient for the $\hat{m}\Psi^\dagger\Psi$ is determined by the soft-pion theorem.

order of the quark mass expansion unless higher order corrections (*e.g.* the coefficient in front of $\hat{m}^2\Psi^\dagger\Psi$) to the action are known.

The electromagnetic form factors of the baryons $F_i(q^2)$ are defined by the expectation values of the electromagnetic current V_μ of the quark fields:

$$\langle B', p' | V_\mu(0) | B, p \rangle = \bar{u}_{B'}(p') \left[\gamma_\mu F_1(q^2) + i\sigma_{\mu\nu} \frac{q^\nu}{2M_N} F_2(q^2) \right] u_B(p) \quad (8)$$

with

$$V_\mu(z) = \bar{\Psi}(z) \gamma_\mu \hat{Q} \Psi(z). \quad (9)$$

M_N denotes the nucleon mass. \hat{Q} designates the charge operator of the quark field $\Psi(z)$

$$\begin{aligned} \hat{Q} &= \begin{pmatrix} \frac{2}{3} & 0 & 0 \\ 0 & -\frac{1}{3} & 0 \\ 0 & 0 & -\frac{1}{3} \end{pmatrix} \\ &= T_3 + \frac{Y}{2}. \end{aligned} \quad (10)$$

T_3 and Y are respectively the third component of the isospin and hypercharge given by the Gell-Mann–Nishijima formula. The q^2 is just the four momentum transfer $q^2 = -Q^2$ with $Q^2 > 0$. Hence, the electromagnetic current V_μ can be decomposed into the third and eighth $SU(3)$ octet currents

$$V_\mu = V_\mu^{(3)} + \frac{1}{\sqrt{3}} V_\mu^{(8)} \quad (11)$$

with

$$\begin{aligned} V_\mu^{(3)} &= \frac{1}{2} \bar{\Psi} \gamma_\mu \lambda^3 \Psi \\ V_\mu^{(8)} &= \frac{1}{2} \bar{\Psi} \gamma_\mu \lambda^8 \Psi. \end{aligned} \quad (12)$$

The electromagnetic form factors $F_i(Q^2)$ can be expressed in terms of the Sachs form factors, $G_E(Q^2)$ and $G_M(Q^2)$:

$$\begin{aligned}
G_E^B(Q^2) &= F_1^B(Q^2) - \frac{Q^2}{4M_N^2} F_2^B(Q^2), \\
G_M^B(Q^2) &= F_1^B(Q^2) + F_2^B(Q^2).
\end{aligned} \tag{13}$$

In the non-relativistic limit ($Q^2 \ll M_N^2$), the Sachs form factors $G_E(Q^2)$ and $G_M(Q^2)$ are related to the time and space components of the electromagnetic current, respectively:

$$\begin{aligned}
\langle B', p' | V_0(0) | B, p \rangle &= G_E^B(Q^2) \\
\langle B', p' | V_i(0) | B, p \rangle &= \frac{1}{2M_N} G_M^B(Q^2) i \epsilon_{ijk} q^j \langle \lambda' | \sigma_k | \lambda \rangle,
\end{aligned} \tag{14}$$

where σ_k stand for Pauli spin matrices. $|\lambda\rangle$ is the corresponding spin state of the baryon.

The matrix elements of the electromagnetic current can be represented by the Euclidean functional integral in our model defined by eq. (1)

$$\begin{aligned}
\langle B', p' | V_\mu(0) | B, p \rangle &= \frac{1}{\mathcal{Z}} \lim_{T \rightarrow \infty} \exp(ip_4 \frac{T}{2} - ip'_4 \frac{T}{2}) \\
&\times \int d^3x d^3y \exp(-i\vec{p}' \cdot \vec{y} + i\vec{p} \cdot \vec{x}) \int \mathcal{D}U \int \mathcal{D}\Psi \int \mathcal{D}\Psi^\dagger \\
&\times J_{B'}(\vec{y}, T/2) \Psi^\dagger(0) \beta \gamma_\mu \hat{Q} \Psi(0) J_B^\dagger(\vec{x}, -T/2) \\
&\times \exp \left[- \int d^4z \Psi^\dagger i D \Psi \right].
\end{aligned} \tag{15}$$

The baryonic states $|B, p\rangle$ and $\langle B', p'|$ are respectively defined by

$$\begin{aligned}
|B, p\rangle &= \lim_{x_4 \rightarrow -\infty} \exp(ip_4 x_4) \frac{1}{\sqrt{\mathcal{Z}}} \int d^3x \exp(i\vec{p} \cdot \vec{x}) J_B^\dagger(\vec{x}, x_4) |0\rangle \\
\langle B', p'| &= \lim_{y_4 \rightarrow +\infty} \exp(-ip'_4 y_4) \frac{1}{\sqrt{\mathcal{Z}}} \int d^3y \exp(-i\vec{p}' \cdot \vec{y}) \langle 0 | J_{B'}(\vec{y}, y_4)
\end{aligned} \tag{16}$$

The baryon current J_B can be constructed from quark fields with the number of colors N_c

$$J_B(x) = \frac{1}{N_c!} \epsilon_{i_1 \dots i_{N_c}} \Gamma_{JJ_3 TT_3 Y}^{\alpha_1 \dots \alpha_{N_c}} \psi_{\alpha_1 i_1}(x) \dots \psi_{\alpha_{N_c} i_{N_c}}(x). \tag{17}$$

$\alpha_1 \dots \alpha_{N_c}$ denote spin-flavor indices, while $i_1 \dots i_{N_c}$ designate color indices. The matrices $\Gamma_{JJ_3 TT_3 Y}^{\alpha_1 \dots \alpha_{N_c}}$ are taken to endow the corresponding current with the quantum numbers $JJ_3 TT_3 Y$.

The J_B^\dagger plays the role of creating the baryon state. With the quark fields being integrated out, eq. (15) can be divided into two separated contributions:

$$\langle B', p' | V_\mu(0) | B, p \rangle = \langle B', p' | V_\mu(0) | B, p \rangle_{val} + \langle B', p' | V_\mu(0) | B, p \rangle_{sea}, \quad (18)$$

where

$$\begin{aligned} \langle B', p' | V_\mu(0) | B, p \rangle_{val} &= \frac{1}{\mathcal{Z}} \Gamma_{J' J_3 T' T_3 Y'}^{\beta_1 \dots \beta_{N_c}} \Gamma_{J J_3 T T_3 Y}^{\alpha_1 \dots \alpha_{N_c} *} \lim_{T \rightarrow \infty} \exp \left(i p_4 \frac{T}{2} - i p'_4 \frac{T}{2} \right) \\ &\times \int d^3 x d^3 y \exp \left(-i \vec{p}' \cdot \vec{y} + i \vec{p} \cdot \vec{x} \right) \\ &\times \int \mathcal{D}U \exp \left(-S_{eff} \right) \sum_{i=1}^{N_c} \beta_i \langle \vec{y}, T/2 | \frac{1}{iD} | 0, t_z \rangle_\gamma [\beta \gamma_\mu \hat{Q}]_{\gamma \gamma'} \\ &\times \gamma' \langle 0, t_z | \frac{1}{iD} | \vec{x}, -T/2 \rangle_{\alpha_i} \prod_{j \neq i}^{N_c} \beta_j \langle \vec{y}, T/2 | \frac{1}{iD} | \vec{x}, -T/2 \rangle_{\alpha_j} \end{aligned} \quad (19)$$

and

$$\begin{aligned} \langle B', p' | V_\mu(0) | B, p \rangle_{sea} &= \frac{1}{\mathcal{Z}} \Gamma_{J' J_3 T' T_3 Y'}^{\beta_1 \dots \beta_{N_c}} \Gamma_{J J_3 T T_3 Y}^{\alpha_1 \dots \alpha_{N_c} *} \lim_{T \rightarrow \infty} \exp \left(i p_4 \frac{T}{2} - i p'_4 \frac{T}{2} \right) \\ &\times \int d^3 x d^3 y \exp \left(-i \vec{p}' \cdot \vec{y} + i \vec{p} \cdot \vec{x} \right) \\ &\times \int \mathcal{D}U \exp \left(-S_{eff} \right) \text{Tr}_{\gamma \lambda c} \langle 0, t_z | \frac{1}{iD} [\beta \gamma_\mu \hat{Q}] | 0, t_z \rangle \\ &\times \prod_{i=1}^{N_c} \beta_i \langle \vec{y}, T/2 | \frac{1}{iD} | \vec{x}, -T/2 \rangle_{\alpha_i}. \end{aligned} \quad (20)$$

S_{eff} is the effective chiral action expressed by

$$S_{eff} = -\text{Sp} \log [\partial_\tau + H(U) + \beta \hat{m} - \beta \bar{m} \mathbf{1}]. \quad (21)$$

Sp stands for the functional trace of the time-independent function.

The integral over bosonic fields can be carried out by the saddle point method in the large N_c limit, choosing the following Ansatz:

$$U = \begin{pmatrix} U_0 & 0 \\ 0 & 1 \end{pmatrix}, \quad (22)$$

where U_0 is the SU(2) chiral background field

$$U_0 = \exp [\vec{n} \cdot \vec{\tau} P(r)]. \quad (23)$$

$P(r)$ denotes the profile function satisfying the boundary condition $P(0) = \pi$ and $P(\infty) = 0$.

In order to find the quantum $1/N_c$ corrections, we have to integrate eqs. (19,20) over small

oscillations of the pseudo-Goldstone field around the saddle point eq. (22). This will not be done except for the zero modes. The corresponding fluctuations of the pion fields are not small and hence cannot be neglected. The zero modes are pertinent to continuous symmetries in our problem. Actually, there are three translational and seven rotational zero modes. We have to take into account the translational zero modes properly in order to evaluate form factors, since the soliton is not invariant under translation and its translational invariance is restored only after integrating over the translational zero modes. The rotational zero modes determine the quantum numbers of baryons [9]. Explicitly, the zero modes are taken into account by considering a slowly *rotating* and *translating* hedgehog:

$$\tilde{U}(\vec{x}, t) = A(t)U(\vec{x} - \vec{Z}(t))A^\dagger(t). \quad (24)$$

$A(t)$ belongs to an $SU(3)$ unitary matrix. The Dirac operator $i\tilde{D}$ in eq. (6) can be written as

$$i\tilde{D} = \left(\partial_\tau + H(U) + A^\dagger(t)\dot{A}(t) - i\beta\dot{\vec{Z}} \cdot \nabla + \beta A^\dagger(t)(\hat{m} - \bar{m}\mathbf{1})A(t) \right). \quad (25)$$

The corresponding collective action is expressed by

$$\begin{aligned} \tilde{S}_{eff} = -N_c \text{Sp} \log & \left[\partial_\tau + H(U) + A^\dagger(t)\dot{A}(t) - i\beta\dot{\vec{Z}} \cdot \nabla \right. \\ & \left. + \beta A^\dagger(t)(\hat{m} - \bar{m}\mathbf{1})A(t) - \beta A^\dagger(t)V_\mu \gamma_\mu \hat{Q}A(t) \right] \end{aligned} \quad (26)$$

with the angular velocity

$$A^\dagger(t)\dot{A}(t) = i\Omega_E = \frac{1}{2}i\Omega_E^a \lambda^a \quad (27)$$

and the velocity of the translational motion

$$\dot{\vec{Z}} = \frac{d}{dt}\vec{Z} \quad (28)$$

The canonical quantization of the $SU(3)$ soliton can be found in Ref. [31,32]. Expanding eq. (26) in powers of angular and translational velocities ($\sim 1/N_c$), we end up with the action for collective coordinates:

$$S_{coll} \approx -N_c \text{Tr} \log iD + S_{rot}[A] + S_{trans}[\vec{Z}] \quad (29)$$

where

$$\begin{aligned} S_{rot}[A] &= \frac{1}{2} I_{ab} \int dt \Omega_a \Omega_b \\ S_{trans}[\vec{Z}] &= \frac{1}{2} M_{cl} \int dt \dot{\vec{Z}} \cdot \dot{\vec{Z}}, \end{aligned} \quad (30)$$

with the moments of inertia I^{ab} calculated in Ref. [23]. M_{cl} is a classical mass of the soliton.

Corresponding collective hamiltonians have a form:

$$\begin{aligned} H_{rot} &= (I^{-1})_{ab} J_a J_b, \\ H_{trans} &= \frac{\vec{P} \cdot \vec{P}}{2M_{cl}}, \end{aligned} \quad (31)$$

where J_a are operators of angular momentum and \vec{P} are momentum operators.

Hence, eq. (19) and eq. (20) can be written in terms of the rotated Dirac operator $i\tilde{D}$ and chiral effective action \tilde{S}_{eff} . The functional integral over the pseudoscalar field U is replaced by the path integral which can be calculated in terms of the eigenstates of the hamiltonian corresponding to the collective action given in eq. (29) and these hamiltonians can be diagonalized in an exact manner. Therefore, eqs. (19,20) can be rewritten as ordinary integrals:

$$\begin{aligned} \langle B', p' | V_\mu(0) | B, p \rangle_{val} &= \frac{1}{\mathcal{Z}} \Gamma_{J' J'_3 T' T'_3 Y'}^{\beta_1 \dots \beta_{N_c}} \Gamma_{J J_3 T T_3 Y}^{\alpha_1 \dots \alpha_{N_c} *} \exp[-((N_c - 1)E_{val} + E_{sea})T] \\ &\times \lim_{T \rightarrow \infty} \int d^3x d^3y \exp(-i\vec{p}' \cdot \vec{y} + i\vec{p} \cdot \vec{x}) \\ &\times \int dA_f dAdA_i d\vec{Z}_f d\vec{Z} d\vec{Z}_i \langle \vec{Z}_f | \exp(-H_{trans}T/2) | \vec{Z} \rangle \\ &\times \langle \vec{Z} | \exp(-H_{trans}T/2) | \vec{Z}_i \rangle \langle A_f | \exp(-H_{rot}T/2) | A \rangle \\ &\times \langle A | \exp(-H_{rot}T/2) | A_i \rangle \\ &\times \sum_{k=1}^{N_c} \mathcal{T} \left[\beta_k \langle \vec{y} - \vec{Z}_f, T/2 | A_f \frac{1}{i\tilde{D}} | -\vec{Z} \rangle_\gamma [A^\dagger \beta \gamma_\mu \hat{Q} A]_{\gamma\gamma'} \right. \\ &\left. \times \gamma' \langle -\vec{Z} | \frac{1}{i\tilde{D}} A_i^\dagger | \vec{x} - \vec{Z}_i, -T/2 \rangle_{\alpha_k} \right], \end{aligned} \quad (32)$$

$$\langle B', p' | V_\mu(0) | B, p \rangle_{sea} = \frac{1}{\mathcal{Z}} \Gamma_{J' J'_3 T' T'_3 Y'}^{\beta_1 \dots \beta_{N_c}} \Gamma_{J J_3 T T_3 Y}^{\alpha_1 \dots \alpha_{N_c} *} \exp[-(N_c E_{val} + E_{sea})T]$$

$$\begin{aligned}
& \times \lim_{T \rightarrow \infty} \int d^3x d^3y \exp(-i\vec{p}' \cdot \vec{y} + i\vec{p} \cdot \vec{x}) \\
& \times \int dA_f dA dA_i d\vec{Z}_f d\vec{Z} d\vec{Z}_i \langle \vec{Z}_f | \exp(-H_{trans}T/2) | \vec{Z} \rangle \\
& \times \langle \vec{Z} | \exp(-H_{trans}T/2) | \vec{Z}_i \rangle \langle A_f | \exp(-H_{rot}T/2) | A \rangle \\
& \times \langle A | \exp(-H_{rot}T/2) | A_i \rangle \\
& \times \mathcal{T} \left[\text{Tr}_{\gamma\lambda c} \langle -\vec{Z} | \frac{1}{i\hat{D}} [A^\dagger \beta \gamma_\mu \hat{Q} A] | -\vec{Z} \rangle_{\gamma\gamma'} \right]. \tag{33}
\end{aligned}$$

$\mathcal{T}[\dots]$ denotes the time-ordered product of collective operators. This is due to the fact that the functional integral corresponds to the matrix elements of the time-ordered products of the collective operators. In particular, the time-ordering is very significant when we consider the magnetic form factors (as in case of the axial constants: see [15,20]), since the spin operator J^a does not commute with the SU(3) rotational unitary matrix $A(t)$. As we integrate over zero modes in the final and initial states, we obtain the translational and rotational corrections of the classical energies of the soliton from the effective actions S_{trans} and S_{rot} . Therefore, introducing the spectral representations of the quark propagator [5] expressed by the eigenfunctions of the Dirac hamiltonian $H(U)$ and making use of relations

$$\int d\vec{Z}_i \langle \vec{Z} | \exp(-S_{trans}) | \vec{Z}_i \rangle f(\vec{x} - \vec{Z}_i) \xrightarrow{T \rightarrow \infty} \langle \vec{Z} | \exp(-S_{trans}) | \vec{x} \rangle \int d^3x' f(\vec{x}'), \tag{34}$$

$$\Gamma_{JJ_3TT_3Y}^{\beta_1 \dots \beta_{N_c}} \int d^3x' \prod_{k=1}^{N_c} [A_f \phi(\vec{x}')]_{\beta_k} = \psi_{(YTT_3)(Y'JJ_3)}^{(8)*}(A_f), \tag{35}$$

$$\Gamma_{JJ_3TT_3Y}^{\alpha_1 \dots \alpha_{N_c}} \int d^3x' \prod_{k=1}^{N_c} [\phi^\dagger(\vec{x}') A_i^\dagger]_{\alpha_k} = \psi_{(YTT_3)(Y'JJ_3)}^{(8)}(A_i), \tag{36}$$

$$\langle A | \exp(-S_{rot}) | A_i \rangle = \sum_{\substack{n \\ (Y'JJ_3) \\ (YTT_3)}} \psi_{(YTT_3)(Y'JJ_3)}^{(n)}(A) \psi_{(YTT_3)(Y'JJ_3)}^{(n)*}(A_i) \exp\left(-\frac{J(J+1)}{2I} T\right), \tag{37}$$

we obtain relatively simple expressions:

$$\begin{aligned}
\langle B', p' | V_\mu(0) | B, p \rangle_{val} &= N_c \int d^3Z \exp(i\vec{q} \cdot \vec{Z}) \int_{\text{SU}(3)} dA \psi_{\mu\nu'}^{(n)*}(A) \psi_{\mu'\nu}^{(n)}(A) \\
&\times \mathcal{T} \left[\mathcal{F}_1^{(\Omega^0)}(A) + \mathcal{F}_2^{(\Omega^1)}(A) + \mathcal{F}_3^{(m_s)}(A) \right] \tag{38}
\end{aligned}$$

$$\begin{aligned}
\langle B', p' | V_\mu(0) | B, p \rangle_{sea} &= N_c \int d^3Z \exp(i\vec{q} \cdot \vec{Z}) \int_{\text{SU}(3)} dA \psi_{\mu\nu'}^{(n)*}(A) \psi_{\mu'\nu}^{(n)}(A) \\
&\times \mathcal{T} \left[\text{Tr} \langle \vec{Z} | \frac{1}{i\hat{D}} [A^\dagger \beta \gamma_\mu \hat{Q} A] | \vec{Z} \rangle \right]. \tag{39}
\end{aligned}$$

Here, we have considered contributions up to the first order of Ω_E , *i.e.* the $1/N_c$ corrections and the linear corrections of the strange quark mass m_s . The mixed term $O(m_s/N_c)$ is relatively small, so that it is neglected [28]. It is performed by the expansion of the propagator $1/i\tilde{D}$ in terms of Ω_E and m_s :

$$\frac{1}{i\tilde{D}} \approx \frac{1}{\partial_\tau + H} + \frac{1}{\partial_\tau + H}(-i\Omega_E)\frac{1}{\partial_\tau + H} + \frac{1}{\partial_\tau + H}(-\beta A^\dagger \hat{m} A)\frac{1}{\partial_\tau + H}. \quad (40)$$

The collective SU(3) octet wave functions $\psi_{\mu'\nu'}^{(n)}(A)$ are identified with the SU(3) Wigner functions

$$\psi_{(YTT_3)(Y'JJ_3)}^{(n)}(A) = \sqrt{\dim(n)}(-1)^{Y'/2+J_3} [\langle Y, T, T_3 | D^{(n)}(A) | -Y', J, -J_3 \rangle]^* \quad (41)$$

as eigenstates of the collective rotational hamiltonian. The functions $\mathcal{F}_i(A)$ are defined as

$$\begin{aligned} \mathcal{F}_1^{(\Omega^0)}(A) &= \langle val | \beta \gamma_\mu \lambda^a | val \rangle D_{Qa}^{(8)}(A) \\ \mathcal{F}_2^{(\Omega^1)}(A) &= - \sum_n \left[\langle val | \lambda^a | n \rangle \langle n | \beta \gamma_\mu \lambda^b | val \rangle i\Omega_E^a(A) D_{Qb}^{(8)}(A) \right. \\ &\quad \left. + \langle val | \beta \gamma_\mu \lambda^b | n \rangle \langle n | \lambda^a | val \rangle D_{Qb}^{(8)}(A) i\Omega_E^a(A) \right] \frac{1}{E_{val} - E_n} \\ \mathcal{F}_3^{(m_s)}(A) &= -(m_0 - \bar{m}) \sum_n \left[\langle val | \beta | n \rangle \langle n | \beta \gamma_\mu \lambda^a | val \rangle D_{Qa}^{(8)}(A) \right. \\ &\quad \left. + \langle val | \beta \gamma_\mu \lambda^a | n \rangle \langle n | \beta | val \rangle D_{Qa}^{(8)}(A) \right] \frac{1}{E_{val} - E_n} \\ &\quad - m_8 \sum_n \left[\langle val | \beta \lambda^a | n \rangle \langle n | \beta \gamma_\mu \lambda^b | val \rangle D_{8a}^{(8)}(A) D_{Qb}^{(8)}(A) \right. \\ &\quad \left. + \langle val | \beta \gamma_\mu \lambda^b | n \rangle \langle n | \beta \lambda^a | val \rangle D_{Qb}^{(8)}(A) D_{8a}^{(8)}(A) \right] \frac{1}{E_{val} - E_n} \end{aligned} \quad (42)$$

$D_{Qa}^{(8)}$ is defined as $\frac{1}{2}(D_{3a}^{(8)} + \frac{1}{\sqrt{3}}D_{8a}^{(8)})$. The collective SU(3) octet wave function in eq. (41) satisfies the orthonormality [33]

$$\int dA \psi_{\mu'\nu'}^{(n')*}(A) \psi_{\mu\nu}^{(n)}(A) = \delta_{n'n} \delta_{\mu'\mu} \delta_{\nu'\nu}. \quad (43)$$

The subscripts $\mu\nu$ of $\psi_{\mu\nu}^{(n)}$ represent $(YTT_3)(Y'JJ_3)$. (n) stands for the irreducible representation of SU(3). Y' is the negative of the right hypercharge constrained by $Y_R = \frac{N_c B}{3} = 1$. Since eq. (39), in particular, its real part diverges, we have to regularize it. We employ the well-known proper time regularization

$$\text{Re}S_{eff} = \frac{1}{2}\text{Tr} \int_0^\infty \frac{du}{u} e^{-uD^\dagger D} \phi(u; \Lambda_i) \quad (44)$$

with

$$\phi(u; \Lambda_i) = \sum_i c_i \theta\left(u - \frac{1}{\Lambda_i^2}\right). \quad (45)$$

The cut-off parameter $\phi(u; \Lambda_i)$ is fixed via reproducing the physical pion decay constant $f_\pi = 93\text{MeV}$ and other mesonic properties [23]. As was done in case of the valence part, we take into account the $1/N_c$ and linear m_s corrections(See appendix A for detail).

Making use of the expansion eq. (40) and the SU(3) octet wave functions and employing the proper-time regularization, we arrive at

$$\begin{aligned} \langle B', p' | V_\mu(0) | B, p \rangle_{val} &= N_c \langle D_{Qa}^{(8)} \rangle_B \mathcal{P}_{\mu;val}^a(\vec{q}) \\ &+ \frac{N_c}{2} \sum_m \left\{ \begin{array}{l} \text{sign}(E_m) \langle [D_{Qa}^{(8)}, i\Omega_E^b] \rangle_B \delta_{\mu i} \\ \langle \{D_{Qa}^{(8)}, i\Omega_E^b\} \rangle_B \delta_{\mu 4} \end{array} \right\} \frac{\mathcal{Q}_{\mu;val,m}^{ab}(\vec{q})}{E_n - E_{val}} \\ &+ \frac{N_c}{2} \sum_m \langle \{D_{Qa}^{(8)}, i\Omega_E^b\} \rangle_B \delta_{\mu i} \frac{\mathcal{Q}_{\mu;val,m}^{ab}(\vec{q})}{E_n - E_{val}} \\ &+ N_c (m_0 - \bar{m}) \sum_m \langle D_{Qa}^{(8)} \rangle_B \delta_{\mu i} \frac{\mathcal{M}_{\mu;val,m}^a(\vec{q})}{E_n - E_{val}} \\ &+ N_c m_8 \sum_m \langle \{D_{Qa}^{(8)}, D_{8b}^{(8)}\} \rangle_B \frac{\mathcal{K}_{\mu;val,m}^{ab}(\vec{q})}{E_n - E_{val}} \end{aligned} \quad (46)$$

$$\begin{aligned} \langle B', p' | V_\mu(0) | B, p \rangle_{sea} &= -\frac{N_c}{2} \sum_m \text{sign}(E_n) \langle D_{Qa}^{(8)} \rangle_B \left\{ \begin{array}{l} \mathcal{R}(E_n) \delta_{\mu i} \\ \delta_{\mu 4} \end{array} \right\} \mathcal{P}_{\mu;n}^a(\vec{q}) \\ &+ \frac{N_c}{4} \sum_{n,m} \left\{ \begin{array}{l} \mathcal{R}_Q(E_n, E_m) \langle [D_{Qa}^{(8)}, i\Omega_E^b] \rangle_B \delta_{\mu i} \\ \mathcal{R}_I(E_n, E_m) \langle \{D_{Qa}^{(8)}, i\Omega_E^b\} \rangle_B \delta_{\mu 4} \end{array} \right\} \mathcal{Q}_{\mu;n,m}^{ab}(\vec{q}) \\ &+ \frac{N_c}{4} \sum_{n,m} \langle \{D_{Qa}^{(8)}, i\Omega_E^b\} \rangle_B \mathcal{R}_M(E_n, E_m) \delta_{\mu i} \mathcal{Q}_{\mu;n,m}^{ab}(\vec{q}) \\ &+ \frac{N_c}{2} (m_0 - \bar{m}) \sum_{n,m} \langle D_{Qa}^{(8)} \rangle_B \mathcal{R}_\beta(E_n, E_m) \mathcal{M}_{\mu;n,m}^a(\vec{q}) \delta_{\mu i} \\ &+ \frac{N_c}{2} m_8 \sum_{n,m} \langle \{D_{Qa}^{(8)}, D_{8b}^{(8)}\} \rangle_B \left\{ \begin{array}{l} \mathcal{R}_\beta(E_n, E_m) \delta_{\mu i} \\ \mathcal{R}_M(E_n, E_m) \delta_{\mu 4} \end{array} \right\} \mathcal{K}_{\mu;n,m}^{ab}(\vec{q}), \end{aligned} \quad (47)$$

where the quark matrix elements are written as

$$\begin{aligned}
\mathcal{P}_{\mu;n}^a(\vec{q}) &= \int d^3x e^{i\vec{q}\cdot\vec{x}} \Psi_n^\dagger(x) \beta \gamma_\mu \lambda^a \Psi_n(x), \\
\mathcal{Q}_{\mu;nm}^{ab}(\vec{q}) &= \int d^3x e^{i\vec{q}\cdot\vec{x}} \int d^3y \Psi_n^\dagger(x) \beta \gamma_\mu \lambda^a \Psi_m(x) \Psi_m^\dagger(y) \lambda^b \Psi_n(y), \\
\mathcal{M}_{\mu;nm}^a(\vec{q}) &= \int d^3x e^{i\vec{q}\cdot\vec{x}} \int d^3y \Psi_n^\dagger(x) \beta \gamma_\mu \lambda^a \Psi_m(x) \Psi_m^\dagger(y) \beta \Psi_n(y), \\
\mathcal{K}_{\mu;nm}^{ab}(\vec{q}) &= \int d^3x e^{i\vec{q}\cdot\vec{x}} \int d^3y \Psi_n^\dagger(x) \beta \gamma_\mu \lambda^a \Psi_m(x) \Psi_m^\dagger(y) \beta \lambda^b \Psi_n(y).
\end{aligned} \tag{48}$$

The regularization functions are given by

$$\begin{aligned}
\mathcal{R}(E_n) &= \int \frac{du}{\sqrt{\pi u}} \phi(u; \Lambda_i) |E_n| e^{-uE_n^2}, \\
\mathcal{R}_{\mathcal{Q}}(E_n, E_m) &= \frac{1}{2\pi} c_i \int_0^1 d\alpha \frac{\alpha(E_n + E_m) - E_m \exp(-[\alpha E_n^2 + (1-\alpha)E_m^2]/\Lambda_i^2)}{\sqrt{\alpha(1-\alpha)} \alpha E_n^2 + (1-\alpha)E_m^2}, \\
\mathcal{R}_I(E_n, E_m) &= -\frac{1}{2\sqrt{\pi}} \int_0^\infty \frac{du}{\sqrt{u}} \phi(u; \Lambda_i) \left[\frac{E_n e^{-uE_n^2} + E_m e^{-uE_m^2}}{E_n + E_m} + \frac{e^{-uE_n^2} - e^{-uE_m^2}}{u(E_n^2 - E_m^2)} \right], \\
\mathcal{R}_{\mathcal{M}}(E_n, E_m) &= \frac{1}{2} \frac{\text{sign}(E_n) - \text{sign}(E_m)}{E_n - E_m}, \\
\mathcal{R}_\beta(E_n, E_m) &= \frac{1}{2\sqrt{\pi}} \int_0^\infty \frac{du}{\sqrt{u}} \phi(u; \Lambda_i) \left[\frac{E_n e^{-uE_n^2} - E_m e^{-uE_m^2}}{E_n - E_m} \right].
\end{aligned} \tag{49}$$

I_i are moments of inertia defined in Ref. [22]. $\langle \rangle_B$ denotes the expectation value of the Wigner D functions in collective space spanned by A . The expectation values of the D functions can be evaluated by SU(3) Clebsch–Gordan coefficients listed in [33,34]. The index μ is the Lorentz index and a and b denote the flavors, whereas i designates the space component of the electromagnetic current. We can here notice that in eq. (47) $1/N_c$ term includes two different commuting relations *i.e.*, the commutator and anti-commutator between the SU(3) Wigner function $D^{(8)}$ and the angular velocity Ω_E of the soliton. This is due to the time-ordering of the operators and the symmetric properties of the quark matrix elements under indices n and m or under G^{γ_5} -parity [35]. If the quark matrix elements are antisymmetric, then the commutator survives, while if they are symmetric, then the anti-commutator does. The quark matrix elements for the electric form factors ($\mu = 4$) are symmetric whereas some of the matrix elements for the magnetic form factors are anti-symmetric. However, note that on the whole the matrix element of the current is symmetric, since the regularization

functions are symmetric under exchange of n and m except for \mathcal{R}_Q .

The regularization functions in eq. (49) are determined in the proper time regularization manifestly except for \mathcal{R}_M which corresponds to the Wess-Zumino terms from the imaginary part of the action. In fact, \mathcal{R}_M is not a regularization function. It is independent of the cut-off parameter Λ .

With SU(3) symmetry explicitly broken by m_s , the collective hamiltonian is no longer SU(3)-symmetric. Therefore, the eigenstates of the hamiltonian are not in a pure octet or decuplet but mixed states. Treating m_s as a perturbation, we can obtain the mixed SU(3) baryonic states:

$$|8, B\rangle = |8, B\rangle + c_{10}^B |\bar{10}, B\rangle + c_{27}^B |27, B\rangle \quad (50)$$

with

$$c_{10}^B = \frac{\sqrt{5}}{15}(\sigma - r_1) \begin{bmatrix} 1 \\ 0 \\ 1 \\ 0 \end{bmatrix} I_2 m_s, c_{27}^B = \frac{1}{75}(3\sigma + r_1 - 4r_2) \begin{bmatrix} \sqrt{6} \\ 3 \\ 2 \\ \sqrt{6} \end{bmatrix} I_2 m_s. \quad (51)$$

in the basis $[N, \Lambda, \Sigma, \Xi]$. Here, B denotes the SU(3) octet baryons with the spin 1/2. The constant σ is related to the SU(2) πN sigma term $\Sigma_{SU(2)} = 3/2(m_u + m_d)\sigma$ and r_i designates K_i/I_i , where K_i stands for the anomalous moments of inertia defined in Ref. [23].

III. THE ELECTRIC PROPERTIES OF THE SU(3) OCTET BARYONS

The electric form factors are easily obtained by the matrix elements of the time component of the electromagnetic current, as was defined in eq. (14). eq. (47) furnishes the final expression of the electric form factor. Since the SU(3) hedgehog solutions are obtained by means of the embedding of the SU(2) hedgehog field U_0 as shown in eq. (22), it is convenient to define the projection operators P_T and P_S

$$P_T = \begin{pmatrix} 1 & 0 & 0 \\ 0 & 1 & 0 \\ 0 & 0 & 0 \end{pmatrix}, \quad P_S = \begin{pmatrix} 0 & 0 & 0 \\ 0 & 0 & 0 \\ 0 & 0 & 1 \end{pmatrix}. \quad (52)$$

Having defined these projection operators, we can separate the pure SU(2) part from the SU(3) which are represented by the collective operators. Utilizing the projection operators and introducing SU(2)_T × U(1)_Y invariant tensors

$$P_T \lambda^a = \begin{cases} \tau^a & \text{if } a = 1, 2, 3 \\ 0 & \text{if } a = 4, 5, 6, 7 \\ 1 & \text{if } a = 8 \end{cases}$$

$$P_T \lambda^a P_S \lambda^b = \left[i(f^{abc} - \epsilon^{abc}) - \frac{1}{\sqrt{3}}(\delta^{ac}\delta^{b8} + \delta^{a8}\delta^{bc}) + d^{abc} \right] \lambda^c, \quad (53)$$

we can find that the quark matrix elements include only the pure SU(2) components with transition matrix elements between the vacuum states with SU(2) flavors and the eigenstates of the one-body Hamiltonian eq. (7). The SU(3) elements only appear in the collective parts. Hence, we can write the expression of the electric form factors

$$G_E^B(\vec{Q}^2) = \frac{N_c}{\sqrt{3}} \langle D_{Q8}^{(8)} \rangle_B \mathcal{B}(\vec{Q}^2) - \langle D_{Qa}^{(8)} J_a \rangle_B \frac{2\mathcal{I}_1(\vec{Q}^2)}{I_1} - \langle D_{Qp}^{(8)} J_p \rangle_B \frac{2\mathcal{I}_2(\vec{Q}^2)}{I_2}$$

$$+ \langle D_{8a}^{(8)} D_{Qa}^{(8)} \rangle_B \frac{4m_s}{I_1 \sqrt{3}} \left(I_1 \mathcal{K}_1(\vec{Q}^2) - \mathcal{I}_1(\vec{Q}^2) K_1 \right)$$

$$+ \langle D_{8p}^{(8)} D_{Qp}^{(8)} \rangle_B \frac{4m_s}{I_2 \sqrt{3}} \left(I_2 \mathcal{K}_2(\vec{Q}^2) - \mathcal{I}_2(\vec{Q}^2) K_2 \right), \quad (54)$$

where

$$\mathcal{B}(\vec{Q}^2) = \int d^3x j_0(Qr) \left[\Psi_{val}^\dagger(x) \Psi_{val}(x) - \frac{1}{2} \sum_n \text{sign}(E_n) \Psi_n^\dagger(x) \Psi_n(x) \right],$$

$$\mathcal{I}_1(\vec{Q}^2) = \frac{N_c}{6} \sum_{n,m} \int d^3x j_0(Qr) \int d^3y \left[\frac{\Psi_n^\dagger(x) \vec{\tau} \Psi_{val}(x) \cdot \Psi_{val}^\dagger(y) \vec{\tau} \Psi_n(y)}{E_n - E_{val}} \right. \\ \left. + \frac{1}{2} \Psi_n^\dagger(x) \vec{\tau} \Psi_m(x) \cdot \Psi_m^\dagger(y) \vec{\tau} \Psi_n(y) \mathcal{R}_{\mathcal{I}}(E_n, E_m) \right],$$

$$\mathcal{I}_2(\vec{Q}^2) = \frac{N_c}{6} \sum_{n,m^0} \int d^3x j_0(Qr) \int d^3y \left[\frac{\Psi_{m^0}^\dagger(x) \Psi_{val}(x) \Psi_{val}^\dagger(y) \Psi_{m^0}(y)}{E_{m^0} - E_{val}} \right. \\ \left. + \frac{1}{2} \Psi_n^\dagger(x) \Psi_{m^0}(x) \Psi_{m^0}^\dagger(y) \Psi_n(y) \mathcal{R}_{\mathcal{I}}(E_n, E_{m^0}) \right],$$

$$\begin{aligned}
\mathcal{K}_1(\vec{Q}^2) &= \frac{N_c}{6} \sum_{n,m} \int d^3x j_0(Qr) \int d^3y \left[\frac{\Psi_n^\dagger(x) \vec{\tau} \Psi_{val}(x) \cdot \Psi_{val}^\dagger(y) \beta \vec{\tau} \Psi_n(y)}{E_n - E_{val}} \right. \\
&\quad \left. + \frac{1}{2} \Psi_n^\dagger(x) \vec{\tau} \Psi_m(x) \cdot \Psi_m^\dagger(y) \beta \vec{\tau} \Psi_n(y) \mathcal{R}_{\mathcal{M}}(E_n, E_m) \right], \\
\mathcal{K}_2(\vec{Q}^2) &= \frac{N_c}{6} \sum_{n,m^0} \int d^3x j_0(Qr) \int d^3y \left[\frac{\Psi_{m^0}^\dagger(x) \Psi_{val}(x) \Psi_{val}^\dagger(y) \beta \Psi_{m^0}(y)}{E_{m^0} - E_{val}} \right. \\
&\quad \left. + \frac{1}{2} \Psi_n^\dagger(x) \Psi_{m^0}(x) \Psi_{m^0}^\dagger(y) \beta \Psi_n(y) \mathcal{R}_{\mathcal{M}}(E_n, E_{m^0}^0) \right] \quad (55)
\end{aligned}$$

with the regularization functions \mathcal{R}_I and $\mathcal{R}_{\mathcal{M}}$ defined in Ee. (49). The subscripts a and p denote the flavor indices $a = 1, 2, 3$ and $p = 4, \dots, 7$, respectively, and m^0 denotes the vacuum state with the SU(2) flavor. $j_0(Qr)$ is the spherical Bessel function of integral order 0. We can see that when $\vec{Q}^2 = 0$ \mathcal{B} becomes the baryon number $B = 1$, while \mathcal{I}_i and \mathcal{K}_i become the usual and the anomalous moments of inertia, respectively. In that case, eq. (54) is reduced to the Gell-Mann–Nishijima formula $Q = T_3 + \frac{1}{2}Y$, using the relation

$$\sum_{a=1}^8 D_{3a}^{(8)} R^a = L_3 = T_3, \quad \sum_{a=1}^8 D_{8a}^{(8)} R^a = L_8 = \frac{1}{2}\sqrt{3}Y. \quad (56)$$

At $\vec{Q}^2 = 0$, the mass corrections do not contribute to the electric form factors, since the fourth and fifth terms in eq. (54) vanish at the zero momentum transfer.

In order to calculate the form factors and other observables numerically, we follow the well-known Kahana and Ripka method [36]. Since the isovector electric charge radii have a pole in the chiral limit, we take the pion mass $m_\pi = 139$ MeV into account. The self-consistent profile function obtained by the Kahana-Ripka method has a good behavior in the solitonic region, but the tail of the pion field is spoiled a little due to the finite size of the radial box when we take into account the pion mass. Hence, at large distances we use the exact Yukawa-type asymptotic behavior of the profile function:

$$P(r) = \alpha \exp(-m_\pi r) \frac{1 + m_\pi r}{r^2}, \quad (57)$$

where α is a constant governing the strength of the pion field. It is determined by matching the self-consistent profile function to the asymptotic tail given in eq. (57) at large distances, *i.e.* about 4 fm. Since the neutron electric form factor, electromagnetic charge radius and

magnetic form factors are very sensitive to the long-range tail, we have to use the larger size of the radial box. Hence, we employ the box size $D \simeq 10$ fm which is large enough to incorporate the long-range part properly.

Figure 1 shows the electric form factor of the proton while Figure 2 draws that of the neutron as a function of Q^2 with the constituent quark mass 370 MeV, 420 MeV and 450 MeV. The empirical data are provided by Ref. [39]. From Figure 1, we can easily find that the proton electric form factor (G_E^p) increases as the constituent quark mass does. For the best fit, we choose the constituent quark mass $M = 420$ MeV as usually done for the other observables. However, the neutron electric form factor (G_E^n) does not show such dependence on the M as that of the proton does. The dependence of G_E^n is not monotonous. As shown in Figure 2, G_E^n with $M = 420$ MeV is greater than those in the case of $M = 370$ MeV and $M = 450$ MeV. At the first glance, it might seem to be strange. However, since G_E^n is a very tiny and sensitive quantity, one should carefully examine each contribution to it. Having scrutinized each contribution, we find that the wave function corrections given by eq.(50) are responsible for the above-mentioned behavior in G_E^n . In particular, the σ appearing in eq.(51) plays a pivotal role of governing the behavior of G_E^n . As M increases, the electric form factors increase but the σ decreases. In the meanwhile, the G_E^n gets an optimal value around 420 MeV.

The contribution of the m_s corrections with the wave function corrections is displayed in Figure 3-4. In fact, the m_s corrections without the collective wave functions modified bring G_E^n down sizably, since the m_s terms $(I_i \mathcal{K}_i(\vec{Q}^2) - \mathcal{I}_i(\vec{Q}^2) K_i)$ diminish electric form factors in general. However, as explained above, the collective wave function corrections are in particular significant in order to improve G_E^n . On the contrary to the case of the G_E^p to which the wave function corrections contribute about 1%, those contributions to G_E^n are strong enough to overcome the m_s corrections. As a result, the total m_s corrections enhance G_E^n about 20% \sim 30% in the small Q^2 region.

More important observables for us are probably electric charge radii which are determined by the behavior of the electric form factors near $Q^2 = 0$ which are defined by

$$\langle r^2 \rangle_E^B = -6 \left. \frac{dG_E^B(Q^2)}{dQ^2} \right|_{Q^2=0}. \quad (58)$$

Using eq. (58), we obtain the electric charge radii of the proton and the neutron $\langle r^2 \rangle_p^{th} = 0.78 \text{ fm}^2$ and $\langle r^2 \rangle_n^{th} = -0.09 \text{ fm}^2$, respectively. The experimental data are $\langle r^2 \rangle_p = 0.74 \text{ fm}^2$ and $\langle r^2 \rangle_n = -0.113 \pm 0.003 \text{ fm}^2$ [44]. We can see that our results are in a good agreement with experimental ones within about 10%.

In dotted curves in Figures 3-4 we show the prediction of the SU(2) model [15]. As for the proton electric form factor, it is comparable to the SU(3), whereas a great discrepancy is observed in case of the neutron electric form factor. This discrepancy can be understood by looking into the electric isospin form factors. Figure 5 shows differences in the electric isospin form factors between the SU(2) and SU(3) model. From Figure 5, we can find that in case of the SU(3) the difference between the isoscalar and isovector form factors are quite small while their sum is comparable. The discrepancy in the neutron form factors lies in this difference between electric isospin form factors. It is partly due to the absence of m_s and terms depending on the I_2 in the SU(2) model and partly due to the different expectation values of the collective operators. In particular, the terms with the I_2 in eq. (54) can be understood as kaonic contributions in the mesonic language [45]. They are relevant to the hidden strangeness having an effect on the nucleon.

We now turn our attention to the other SU(3) hyperons. In Figures 6-7 we present the electric form factors for the SU(3) octet hyperons. Figure 6 draws those of charged hyperons while Figure 7 displays those of neutral ones. Without m_s correction, we could observe U -spin symmetry expressed by

$$\begin{aligned} G_{E,M}^p &= G_{E,M}^{\Sigma^+}, & G_{E,M}^{\Sigma^-} &= G_{E,M}^{\Xi^-}, \\ G_{E,M}^n &= G_{E,M}^{\Xi^0}, & G_{E,M}^\Lambda &= -G_{E,M}^{\Sigma^0}. \end{aligned} \quad (59)$$

Figures 6-7 show us SU(3) symmetry breaking arising from the m_s correction. In case of the charged octet baryons the SU(3) splitting of the electric form factors are rather small while it is quite visible for the neutral ones. The predicted electric charge radii for different

baryons are listed in table 1, compared with the SU(3) Skyrme model with pseudoscalar vector mesons [37].

IV. THE MAGNETIC PROPERTIES OF THE SU(3) OCTET BARYONS

The space components of the electromagnetic current is responsible for the magnetic form factors. As used in case of the electric form factor, we again make use of the projection operators given in eq. (52) and SU(2)_T × U(1)_Y invariant tensors, so that we obtain the expression of $G_M^B(\vec{Q}^2)$:

$$\begin{aligned}
G_M^B(\vec{Q}^2) = & \frac{M_N}{|\vec{Q}|} \left[\langle D_{Q3}^{(8)} \rangle_B \left(\mathcal{Q}_0(\vec{Q}^2) + \frac{\mathcal{Q}_1(\vec{Q}^2)}{I_1} + \frac{\mathcal{Q}_2(\vec{Q}^2)}{I_2} \right) \right. \\
& - \langle D_{Q8}^{(8)} J_3 \rangle_B \frac{\mathcal{X}_1(\vec{Q}^2)}{\sqrt{3}I_1} - \langle d_{3pq} D_{Qp}^{(8)} J_q \rangle_B \delta_{pq} \frac{\mathcal{X}_2(\vec{Q}^2)}{I_2} \\
& + 2m_s \langle (D_{88}^{(8)} - 1) D_{Q3}^{(8)} \rangle_B \mathcal{M}_0(\vec{Q}^2) \\
& + m_s \langle D_{83}^{(8)} D_{Q8}^{(8)} \rangle_B \left(2\mathcal{M}_1(\vec{Q}^2) - \frac{2}{3}r_1 \mathcal{X}_1(\vec{Q}^2) \right) \\
& \left. + m_s \sqrt{3} \langle d_{3pq} D_{8p}^{(8)} D_{Qq}^{(8)} \rangle_B \delta_{pq} \left(2\mathcal{M}_2(\vec{Q}^2) - \frac{2}{3}r_2 \mathcal{X}_2(\vec{Q}^2) \right) \right], \tag{60}
\end{aligned}$$

where

$$\begin{aligned}
\mathcal{Q}_0(\vec{Q}^2) = & N_c \int d^3x j_1(qr) \left[\Psi_{val}^\dagger(x) \gamma_5 \{ \hat{r} \times \vec{\sigma} \} \cdot \vec{\tau} \Psi_{val}(x) \right. \\
& \left. - \frac{1}{2} \sum_n \text{sign}(E_n) \Psi_n^\dagger(x) \gamma_5 \{ \hat{r} \times \vec{\sigma} \} \cdot \vec{\tau} \Psi_n(x) \mathcal{R}(E_n) \right], \\
\mathcal{Q}_1(\vec{Q}^2) = & \frac{iN_c}{2} \sum_n \int d^3x j_1(qr) \int d^3y \\
& \times \left[\text{sign}(E_n) \frac{\Psi_n^\dagger(x) \gamma_5 \{ \hat{r} \times \vec{\sigma} \} \times \vec{\tau} \Psi_{val}(x) \cdot \Psi_{val}^\dagger(y) \vec{\tau} \Psi_n(y)}{E_n - E_{val}} \right. \\
& \left. + \frac{1}{2} \sum_m \Psi_n^\dagger(x) \gamma_5 \{ \hat{r} \times \vec{\sigma} \} \times \vec{\tau} \Psi_m(x) \cdot \Psi_m^\dagger(y) \vec{\tau} \Psi_n(y) \mathcal{R}_Q(E_n, E_m) \right], \\
\mathcal{Q}_2(\vec{Q}^2) = & \frac{N_c}{2} \sum_{m^0} \int d^3x j_1(qr) \int d^3y \\
& \times \left[\text{sign}(E_{m^0}) \frac{\Psi_{m^0}^\dagger(x) \gamma_5 \{ \hat{r} \times \vec{\sigma} \} \cdot \vec{\tau} \Psi_{val}(x) \Psi_{val}^\dagger(y) \Psi_{m^0}(y)}{E_{m^0} - E_{val}} \right. \\
& \left. + \sum_n \Psi_n^\dagger(x) \gamma_5 \{ \hat{r} \times \vec{\sigma} \} \cdot \vec{\tau} \Psi_{m^0}(x) \Psi_{m^0}^\dagger(y) \Psi_n(y) \mathcal{R}_Q(E_n, E_{m^0}) \right],
\end{aligned}$$

$$\begin{aligned}
\mathcal{X}_1(\vec{Q}^2) &= N_c \sum_n \int d^3x j_1(qr) \int d^3y \left[\frac{\Psi_n^\dagger(x) \gamma_5 \{\hat{r} \times \vec{\sigma}\} \Psi_{val}(x) \cdot \Psi_{val}^\dagger(y) \vec{\tau} \Psi_n(y)}{E_n - E_{val}} \right. \\
&\quad \left. + \frac{1}{2} \sum_m \Psi_n^\dagger(x) \gamma_5 \{\hat{r} \times \vec{\sigma}\} \Psi_m(x) \cdot \Psi_m^\dagger(y) \vec{\tau} \Psi_n(y) \mathcal{R}_{\mathcal{M}}(E_n, E_m) \right], \\
\mathcal{X}_2(\vec{Q}^2) &= N_c \sum_{m^0} \int d^3x j_1(qr) \int d^3y \left[\frac{\Psi_{m^0}^\dagger(x) \gamma_5 \{\hat{r} \times \vec{\sigma}\} \cdot \vec{\tau} \Psi_{val}(x) \Psi_{val}^\dagger(y) \Psi_{m^0}(y)}{E_{m^0} - E_{val}} \right. \\
&\quad \left. + \sum_n \Psi_n^\dagger(x) \gamma_5 \{\hat{r} \times \vec{\sigma}\} \cdot \vec{\tau} \Psi_{m^0}(x) \Psi_{m^0}^\dagger(y) \Psi_n(y) \mathcal{R}_{\mathcal{M}}(E_n, E_{m^0}) \right], \\
\mathcal{M}_0(\vec{Q}^2) &= \frac{N_c}{3} \sum_n \int d^3x j_1(qr) \int d^3y \left[\frac{\Psi_n^\dagger(x) \gamma_5 \{\hat{r} \times \vec{\sigma}\} \cdot \vec{\tau} \Psi_{val}(x) \Psi_{val}^\dagger(y) \beta \Psi_n(y)}{E_n - E_{val}} \right. \\
&\quad \left. + \frac{1}{2} \sum_m \Psi_n^\dagger(x) \gamma_5 \{\hat{r} \times \vec{\sigma}\} \cdot \vec{\tau} \Psi_m(x) \Psi_m^\dagger(y) \beta \Psi_n(y) \mathcal{R}_\beta(E_n, E_m) \right], \\
\mathcal{M}_1(\vec{Q}^2) &= \frac{N_c}{3} \sum_n \int d^3x j_1(qr) \int d^3y \\
&\quad \times \left[\frac{\Psi_n^\dagger(x) \gamma_5 \{\hat{r} \times \vec{\sigma}\} \Psi_{val}(x) \cdot \Psi_{val}^\dagger(y) \beta \vec{\tau} \Psi_n(y)}{E_n - E_{val}} \right. \\
&\quad \left. + \frac{1}{2} \sum_m \Psi_n^\dagger(x) \gamma_5 \{\hat{r} \times \vec{\sigma}\} \Psi_m(x) \cdot \Psi_m^\dagger(y) \beta \vec{\tau} \Psi_n(y) \mathcal{R}_\beta(E_n, E_m) \right], \\
\mathcal{M}_2(\vec{Q}^2) &= \frac{N_c}{3} \sum_{m^0} \int d^3x j_1(qr) \int d^3y \\
&\quad \times \left[\frac{\Psi_{m^0}^\dagger(x) \gamma_5 \{\hat{r} \times \vec{\sigma}\} \cdot \vec{\tau} \Psi_{val}(x) \Psi_{val}^\dagger(y) \beta \Psi_{m^0}(y)}{E_{m^0} - E_{val}} \right. \\
&\quad \left. + \sum_n \Psi_n^\dagger(x) \gamma_5 \{\hat{r} \times \vec{\sigma}\} \cdot \vec{\tau} \Psi_{m^0}(x) \Psi_{m^0}^\dagger(y) \beta \Psi_n(y) \mathcal{R}_\beta(E_n, E_{m^0}) \right]. \tag{61}
\end{aligned}$$

The regularization functions \mathcal{R} , \mathcal{R}_Q , $\mathcal{R}_{\mathcal{M}}$ and \mathcal{R}_β are defined in eq. (49). The subscripts p and q in eq. (60) designate flavor indices from 4 to 7. The m^0 in the summation stands for the vacuum states with the SU(2) flavor. r_i is K_i/I_i for short. As we can see from the densities for the magnetic form factors in eq. (61), they are pure SU(2) quantities. The SU(3) components are only found in the collective operators in eq. (60). Therefore, it is straightforward to calculate eq. (60) numerically. To make sure, we have compared the density of each contribution with the corresponding density in the gradient expansion given in appendix B. As the soliton size increases, our expressions converge to those of the gradient expansion.

The nucleon magnetic form factors are displayed in Figures 8-9, as the constituent quark

mass is varied from $M = 370$ to $M = 450\text{MeV}$. In contrast to the case of the electric form factors, the dependence of the magnetic form factors on the constituent quark mass is not linear. Up to around $Q^2 = 0.2\text{GeV}^2$ in case of the proton ($Q^2 = 0.4\text{GeV}^2$ for the neutron), smaller constituent quark masses are more contributive to the magnetic form factors. However, as Q^2 increases, the dependence on the constituent quark mass undergoes a change, *i.e.* the greater constituent quark masses contribute more to the magnetic form factors. In fact, we can reach the empirical data in the vicinity of $Q^2 = 0$ with $M = 370\text{MeV}$, we reproduce roughly the correct momentum-dependence. We select $M = 420\text{MeV}$ for the best fit to be consistent with all observables in this paper.

Figures 10-11 present the contribution of the strange quark mass. On the contrary to the electric form factors, the m_s correction enhances the magnetic form factors about 5% to 10%. In particular, it is of great significance for the neutron magnetic form factor in fitting the empirical data as shown in Figure 11. Our theoretical magnetic form factors are in a good agreement with the empirical data within about 15% like the other quantities.

Table 2 shows each contribution of the rotational $1/N_c$ and m_s corrections to the magnetic moments, *i.e.* $G_M^B(Q^2)$ at $Q^2 = 0$ (in Ref. [28], the magnetic moments are discussed in detail). Our results are compared with the SU(3) Skyrme model with pseudoscalar vector meson [37]. Figures 12-13 display the magnetic form factors of the charged and neutral octet baryons, respectively. The explicit breaking of U spin symmetry in the magnetic form factors are observed. The corresponding magnetic charge radii are defined by

$$\langle r^2 \rangle_M^B = -\frac{6}{\mu_B} \left. \frac{dG_M^B(Q^2)}{dQ^2} \right|_{Q^2=0}. \quad (62)$$

Their numerical results are listed in table 3. The results for the nucleon are in a good agreement with the experimental data.

V. SUMMARY AND CONCLUSION

The aim of this work has been to investigate the electromagnetic form factors of the SU(3) octet baryons and related quantities such as electromagnetic charge radii and magnetic mo-

ments in the SU(3) semibosonized NJL model. Starting from the effective chiral action, we have expressed the matrix elements of electromagnetic current in the model. When quantizing the soliton, the contributions arising from the non-commutativity of collective operators was considered. It gives a non-zero contribution of the rotational $1/N_c$ corrections. The m_s corrections are treated perturbatively, the collective wave function correction being taken heed of. The octet states of the baryon are mixed with higher irreducible representations due to m_s .

The parameters of the model, including the cut-off, are adjusted to $m_\pi = 139\text{MeV}$ and $f_\pi = 93\text{MeV}$. The only parameter we have in the model is the constituent quark mass M which is fixed to $M = 420\text{ MeV}$ by the mass splitting of the SU(3) baryons. The electric form factor of the proton is in an excellent agreement with the empirical data. As far as the electric form factor of the neutron is concerned, it is well known that there are large uncertainties in extracting it from experiments [42]. However, compared to ref. [43], our result is found to be in a remarkable agreement with it. The electric charge radii of the nucleon are also obtained in a good agreement with the experimental result within about 10%.

We also evaluated electric and magnetic form factors of all other members of the SU(3) baryon octet. The magnetic moments are in a good agreement with the experimental data. As far as the Q^2 -dependence is concerned, since there are no experimental data available, these numbers are predictions. In all cases the m_s corrections are about 10%.

Electromagnetic form factors of the baryons are used in order to extract strange form factors from the experimental data. The evaluation of these quantities and of semileptonic and mesonic decays of hyperons will be the next steps in our research.

ACKNOWLEDGEMENT

We would like to thank Ch. Christov, P. Pobylitsa, M. Praszalowicz, and T. Watabe for fruitful discussions and critical comments. This work has partly been supported by the

BMFT, the DFG and the COSY–Project (Jülich). The work of M.P. is supported in part by grant INTAS-93-0283.

APPENDIX A: THE DERIVATION OF THE REGULARIZATION

In this appendix, we shall give an explicit derivation of the regularized Ω^0 and Ω^1 contributions to the electromagnetic form factors. We make use of the proper-time regularization scheme. We can see that the procedure is very similar to the case of the axial constants [20]. Note that the non-anomalous part is regularized. As is written in eq. (44), the regularized effective action is expressed as

$$\text{Re}S_{eff} = \text{Sp} \int \frac{du}{u} \phi(u; \Lambda_i) \exp(-uDD^\dagger), \quad (\text{A1})$$

where

$$\begin{aligned} D &= \partial_\tau + H + i\Omega_E + \beta A^\dagger \hat{Q}A - iA_4 A^\dagger \hat{Q}A - \alpha_k A_k A^\dagger \hat{Q}A \\ D^\dagger &= -\partial_\tau + H - i\Omega_E + \beta A^\dagger \hat{Q}A + iA_4 A^\dagger \hat{Q}A - \alpha_k A_k A^\dagger \hat{Q}A. \end{aligned} \quad (\text{A2})$$

Hence,

$$\begin{aligned} DD^\dagger &= W_0(A_\mu^0, \Omega^0, m^0) + W_1(A_\mu^1, \Omega^0, m^0) + W_2(A_\mu^1, \Omega^1) \\ &+ W_3(A_\mu^0, \Omega^1) + W_4(m^1) + O(\Omega^1, m^1) + O(\Omega^2) + O(m^2) \end{aligned} \quad (\text{A3})$$

with

$$\begin{aligned} W_0 &= -\partial_\tau^2 + H_E^2 \\ W_1 &= i\{A_4 A^\dagger \hat{Q}A, \partial_\tau\} - [\alpha_k A_k A^\dagger \hat{Q}A, \partial_\tau] \\ &\quad - i[H_E, A_4 A^\dagger \hat{Q}A] - \{H_E, \alpha_k A_k A^\dagger \hat{Q}A\} \\ W_2 &= -\{\Omega_E, A_4 A^\dagger \hat{Q}A\} + i[\Omega_E, \alpha_k A_k A^\dagger \hat{Q}A] \\ W_3 &= -i\{\Omega_E, \partial_\tau\} + i[H_E, \Omega_E] \\ W_4 &= [\beta A^\dagger \hat{m}A, \partial_\tau] + \{H_E, \beta A^\dagger \hat{m}A\} \\ &\quad - i[\beta A^\dagger \hat{m}A, A_4 A^\dagger \hat{Q}A] + \{\beta A^\dagger \hat{m}A, \alpha_k A_k A^\dagger \hat{Q}A\}. \end{aligned} \quad (\text{A4})$$

The terms of higher orders in Ω and \hat{m} and of $\Omega \cdot \hat{m}$ are neglected, since they are believed to be very tiny.

Taking advantage of the Feynman-Schwinger-Dyson formula, we can expand $\exp(-uW)$ around W_0 :

$$\begin{aligned}
\exp(-uW) &= \exp(-uW_0) \\
&- u \int_0^1 d\alpha \exp(-u\alpha W_0)[W - W_0] \exp(-u(1-\alpha)W_0) \\
&+ u^2 \int_0^1 d\beta \int_0^{1-\beta} \exp(-u\alpha W_0)[W - W_0] \times \\
&\times \exp(-u\beta W_0)[W - W_0] \exp(-u(1-\alpha-\beta)W_0) \\
&+ \dots
\end{aligned} \tag{A5}$$

First, we shall consider in case of the electric form factor. The lowest order contribution of Ω_E vanishes. The sea contribution of Ω_E^0 comes only from the imaginary part of the effective action. As for the next order of Ω_E , we need W_2 and $W_1 \cdot W_3$. After some manipulations, we obtain

$$\begin{aligned}
\langle B, p' | V_0(0) | B, p \rangle^{\Omega^1} &= \frac{N_c}{4} \sum_{nm} R_I(E_n, E_m) \langle \{ D_{Qa}^{(8)}, i\Omega_E^b \} \rangle_B \times \\
&\times \int d^3x e^{i\vec{q}\cdot\vec{x}} \int d^3y \Psi_n^\dagger(x) \lambda^a \Psi_m(x) \Psi_m^\dagger(y) \lambda^b \Psi_n(y).
\end{aligned} \tag{A6}$$

The m_s correction due to W_4 and $W_4 \cdot W_1$ vanishes like Ω^0 contribution. The m_s correction arises only from the quantization of $i\Omega_E$ [23].

The regularization of the magnetic form factor is more involved due to the time-ordering of collective operators. Here, we need only the term $-A_k \{ H_E, \alpha_k A^\dagger \hat{Q} A \}$ for the lowest order contribution:

$$\begin{aligned}
\langle B, p' | V_i(0) | B, p \rangle^{\Omega^0} &= \frac{1}{2} \frac{\delta}{\delta A_i} \text{Sp} \int du \phi(u; \Lambda_i) \int_0^1 d\alpha \exp(-u\alpha W_0) \\
&\times A_k \{ H_E, \alpha_k A^\dagger \hat{Q} A \} \exp(-u(1-\alpha)W_0) \\
&= \frac{N_c}{2} D_{Qa}^{(8)} \sum_n \langle n | \alpha_i \lambda^a | n \rangle R(E_n),
\end{aligned} \tag{A7}$$

where $R(E_n)$ is defined in eq. (49).

As a next step, we proceed to evaluate the Ω_E^1 correction to the magnetic form factor.

It is tedious but straightforward:

$$\langle B, p' | V_i(0) | B, p \rangle^{\Omega^1} = \frac{\delta}{\delta A_i} (X_1[A_k] + X_2[A_k]) |_{A_k=0}, \quad (\text{A8})$$

where

$$\begin{aligned} X_1[A_k] &= \frac{1}{2} \text{Sp} \int du \phi(u; \Lambda_i) \int_0^1 d\alpha \exp(-u\alpha W_0) \\ &\quad \times W_2[A_k] \exp(-u(1-\alpha)W_0), \end{aligned} \quad (\text{A9})$$

$$\begin{aligned} X_2[A_k] &= \frac{1}{2} \text{Sp} \int du \phi(u; \Lambda_i) \int_0^1 d\beta \int_0^{1-\beta} d\alpha \exp(-u\alpha W_0) \\ &\quad \times (W_1[A_k] + W_3[A_k]) \exp(-u\beta W_0) (W_1[A_k] + W_3[A_k]) \\ &\quad \exp(-u(1-\alpha-\beta)W_0). \end{aligned} \quad (\text{A10})$$

The terms including $W_1 \cdot W_1$ and $W_3 \cdot W_3$ vanish. The first term $\frac{\delta}{\delta A_i} X_1[A_k]$ is obtained to be

$$\begin{aligned} \frac{\delta}{\delta A_i} X_1[A_k] &= \frac{-i}{16} N_c \sum_{n,m} \sqrt{\frac{u}{\pi}} (e^{-uE_n^2} - e^{-uE_m^2}) \{i\Omega_E^a, D_{Qb}^{(8)}\} \\ &\quad \langle n | \lambda^a | m \rangle \langle m | \alpha_i \lambda^b | m \rangle. \end{aligned} \quad (\text{A11})$$

The second term is as follows:

$$\begin{aligned} \frac{\delta}{\delta A_i} X_2[A_k] &= -u \frac{iN_c}{8\pi} \sum_{n,m} \int_0^1 d\beta e^{-u[\beta E_m^2 + (1-\beta)E_n^2]} \\ &\quad [\beta E_m - (1-\beta)E_n] \frac{1}{\sqrt{\beta(1-\beta)}} [i\Omega_E^a, D_{Qb}] \\ &\quad \langle n | \lambda^a | m \rangle \langle m | \alpha_i \lambda^b | n \rangle \\ &\quad + \frac{i}{16} N_c \sum_{n,m} \sqrt{\frac{u}{\pi}} (e^{-uE_n^2} - e^{-uE_m^2}) \{i\Omega_E^a, D_{Qb}^{(8)}\} \\ &\quad \langle n | \lambda^a | m \rangle \langle m | \alpha_i \lambda^b | n \rangle. \end{aligned} \quad (\text{A12})$$

The second part of eq. (A12) is cancelled by $\frac{\delta}{\delta A_i} X_1[A_k]$, so that we have

$$\begin{aligned} \langle B, p' | V_i(0) | B, p \rangle^{\Omega^1} &= -u \frac{iN_c}{8\pi} \sum_{n,m} \int_0^1 d\beta e^{-u[\beta E_m^2 + (1-\beta)E_n^2]} \\ &\quad [\beta E_m - (1-\beta)E_n] \frac{1}{\sqrt{\beta(1-\beta)}} [i\Omega_E^a, D_{Qb}] \\ &\quad \langle n | \lambda^a | m \rangle \langle m | \alpha_i \lambda^b | n \rangle. \end{aligned} \quad (\text{A13})$$

Having integrated over β , we obtain

$$\langle B, p' | V_i(0) | B, p \rangle^{\Omega^1} = -\frac{N_c}{4} \sum_m \langle [D_{Qa}^{(8)}, J_b] \rangle_B \langle n | \lambda^a | m \rangle \langle m | \alpha_i \lambda^b | n \rangle \mathcal{R}_Q(E_n, E_m), \quad (\text{A14})$$

where \mathcal{R}_Q is defined in eq. (49).

APPENDIX B: THE GRADIENT EXPANSION OF THE MAGNETIC MOMENTS

It is well known that the exact expressions for the magnetic moments can be expanded in powers of gradients of the chiral fields [48]. In this way the quark determinant gives terms, which are quite similar to the Skyrme model expressions [37]. An important difference is however the contributions of order Ω^1 from the real part of the action. In the present case we obtain

$$\begin{aligned} \mu_B = & -2M_n \int dr r^2 \sin^2 \theta \langle D_{Q3} \rangle_B \left[\frac{8\pi}{3} f_\pi^2 + \frac{1}{3} \frac{M_u}{4I_1} + \frac{1}{3} \frac{M_u}{8I_2} \right] \\ & + \frac{4}{9\pi} \int dr r^2 \sin^2 \theta \theta' \left[\frac{-\langle d_{3pp} D_{Qp} J_p \rangle_B}{I_2} - \frac{\langle D_{Q8} J_3 \rangle_B}{I_1 \sqrt{3}} \right]. \end{aligned} \quad (\text{B1})$$

Our numerical densities for the electromagnetic form factors are compared with those obtained from the gradient expansion in order to warrant the calculation.

REFERENCES

- [1] S. Kahana, G. Ripka and V. Soni, *Nucl. Phys.* **A415** (1984) 351.
- [2] M.S. Birse and M.K. Banerjee, *Phys. Lett.* **136B** (1984)
- [3] V. Soni, *Phys. Lett.* **183B** (1987) 91.
- [4] D. Diakonov and V. Petrov, *Nucl. Phys.* **B272** (1986) 457
- [5] D. Diakonov, V. Petrov and P. Pobylitsa, *Nucl. Phys.* **B272** (1988) 809
- [6] H. Reinhardt and R. Wünsch, *Phys. Lett.* **215B** (1988) 577.
- [7] Th. Meißner, F. Grümmer and K. Goeke, *Phys. Lett.* **227B** (1989) 296.
- [8] M. Wakamatsu and H. Yoshiki, *Nucl. Phys.* **A524** (1991) 561.
- [9] G.S. Adkins, C.R. Nappi and E. Witten, *Nucl. Phys.* **B228** (1983) 552.
- [10] P. Ring and P. Schuck, *The Nuclear Many-Body Problem*, Springer-Verlag, New-York, (1980).
- [11] K. Goeke, A.Z. Górski, F. Grümmer, Th. Meißner, H. Reinhardt and R. Wünsch, *Phys. Lett.* **256B** (1991)321.
- [12] M. Wakamatsu and T. Watabe, *Phys. Lett.* **312B** (1993) 184.
- [13] C.V. Christov, A. Blotz, K. Goeke, P. Pobylitsa, V. Petrov, M. Wakamatsu, and T. Watabe, *Phys. Lett.* **325B** (1994) 467.
- [14] M. Wakamatsu, *Phys. Rev.* **D46** (1992) 3762.
- [15] Ch. Christov, A.Z. Górski, K. Goeke and P.V. Pobylitsa, RUB-TPII-2/94, *Nucl. Phys.* **A** in print (1994)
- [16] A. Blotz, *Ph.D. thesis*, Ruhr-Universität Bochum, (1994).
- [17] H.-C. Kim, A. Blotz, C. Schneider and K. Goeke, RUB-TPII-18/95, (1995)

- [18] A. Blotz, Praszalowicz and K. Goeke, *Acta Phys. Polon.* **B35** (1994) 1443.
- [19] H.-C. Kim, T. Watabe, and K. Goeke, RUB-TPII-11/95 [hep-ph/9506344], (1995)
- [20] A. Blotz, M. Praszalowicz and K. Goeke, *Phys. Lett.* **B317** (1994) 195.
- [21] A. Blotz, M. Praszalowicz and K. Goeke, RUB-TPII-41/93, [hep-ph/9403314] (1993).
- [22] A. Blotz, D. Diakonov, K. Goeke, N.W. Park, V. Petrov and P.V. Pobylitsa, *Phys. Lett.* **B287** (1992) 29.
- [23] A. Blotz, D. Diakonov, K. Goeke, N.W. Park, V. Petrov and P.V. Pobylitsa, *Nucl.Phys.* **A555** (1993) 765.
- [24] H. Weigel, R. Alkofer and H. Reinhardt, *Nucl. Phys.* **B387** (1992) 638.
- [25] A. Blotz, M.V. Polyakov, and K. Goeke, *Phys. Lett.* **302B** (1993) 151.
- [26] A. Blotz, M. Praszalowicz and K. Goeke, *Phys. Lett.* **317B** (1993) 195.
- [27] M. Praszalowicz, A. Blotz and K. Goeke *Phys. Rev.* **D47** (1993) 1127.
- [28] H.-C. Kim, M. Polyakov, A. Blotz, and K. Goeke, RUB-TPII-6/95 [hep-ph/9506422], (1995).
- [29] R. Ball, *Phys. Rep.* **182** (1989) 1.
- [30] C. Itzykson and J.-B. Zuber, *Quantum Field Theory*, McGraw-Hill, New York (1980).
- [31] E. Guadagnini, *Nucl. Phys.* **B236** (1984) 35.
- [32] N. Toyota, *Prog. Theor. Phys.* **77** (1987) 688.
- [33] J.J. de Swart, *Rev. Mod. Phys.* **35** (1963) 916.
- [34] P. McNamee, S.J. and F. Chilton, *Rev. Mod. Phys.* **36** (1964) 1005.
- [35] P. Pobylitsa, *Private communication*.

- [36] S. Kahana and G. Ripka, *Nucl. Phys.* **A429** (1984) 462.
- [37] N.W. Park and H. Weigel, *Nucl. Phys.* **A541** (1992) 453.
- [38] G. Höhler *et al.*, *Nucl. Phys.* **B114** (1976) 505.
- [39] S. Platchkov *et al.*, *Nucl. Phys.* **A510** (1990) 740.
- [40] C.E. Jones-Woodward *et al.*, *Phys. Rev.* **C44** (1991) R571.
- [41] A.K. Thompson *et al.*, *Phys. Rev. Lett.* **68** (1992) 2901.
- [42] T. Eden *et al.*, *Phys. Rev.* **C50** (1994) R1749.
- [43] M. Meyerhoff *et al.*, *Phys. Lett.* **B327** (1994) 201.
- [44] S. Kopecky, P. Riehs, J.A. Harvey and N.W. Hill, *Phys. Rev. Lett.* **74** (1995) 2427.
- [45] T. Watabe, H.-C. Kim, and K. Goeke, RUB-TPII-17/95, [[hep-ph/9507318](#)] (1995).
- [46] Particle Data Group, *Phys. Rev.* **D50** (1994) 1218.
- [47] E.E.W. Bruins *et al.*, *Phys. Rev. Lett.* **75** (1995) 21.
- [48] J.R. Aitchison and C. Frazer, *Phys. Rev.* **D31** (1985) 2608.

TABLES

TABLE I. The electric charge radii of the SU(3) octet baryons predicted by our model compared to the evaluation from the Skyrme model by Park and Weigel [37] and the experimental numbers. The constituent quark mass is fixed to $M = 420$ MeV.

Baryons	Our model	Park & Weigel	Experiment
p	0.78	1.20	0.74
n	-0.09	-0.15	-0.11
Λ	-0.04	-0.06	-
Σ^+	0.79	1.20	-
Σ^0	0.02	-0.01	-
Σ^-	-0.75	-1.21	-
Ξ^0	-0.06	-0.10	-
Ξ^-	-0.72	-1.21	-

TABLE II. The magnetic moments of the SU(3) octet baryons predicted by our model. Each contribution is listed from the leading order. The results are also compared with the Skyrme model of Park and Weigel [37]. The experimental data for the magnetic moments are taken from Ref.[45]. Our final values are given by $\mu_B(\Omega^1, m_s^1)$. The constituent quark mass is fixed to $M = 420$ MeV.

Baryons	$\mu_B(\Omega^0, m_s^0)$	$\mu_B(\Omega^1, m_s^0)$	$\mu_B(\Omega^1, m_s^1)$	Park & Weigel	Exp.
p	1.01	2.27	2.39	2.36	2.79
n	-0.75	-1.55	-1.76	-1.87	-1.91
Λ	-0.38	-0.78	-0.77	-0.60	-0.61
Σ^+	1.01	2.27	2.42	2.41	2.46
Σ^0	0.38	0.78	0.75	0.66	-
Σ^-	-0.25	-0.71	-0.92	-1.10	-1.16
Ξ^0	-0.75	-1.55	-1.64	-1.96	-1.25
Ξ^-	-0.25	-0.71	-0.68	-0.84	-0.65
$ \Sigma^0 \rightarrow \Lambda $	0.65	1.34	1.51	1.74	1.61

TABLE III. The magnetic charge radii of the SU(3) octet baryons predicted by our model compared with the Skyrme model of Park and Weigel [37]. The constituent quark mass is fixed to $M = 420$ MeV.

Baryons	Our model	Park & Weigel	Experiment
p	0.70	0.94	0.74
n	0.78	0.94	0.77
Λ	0.70	0.78	–
Σ^+	0.71	0.96	–
Σ^0	0.70	0.86	–
Σ^-	0.74	1.07	–
Ξ^0	0.75	0.90	–
Ξ^-	0.51	0.84	–

Figure Captions

Fig. 1: The proton electric formfactor as a function of Q^2 : The dashed curve corresponds to the constituent quark mass $M = 370\text{MeV}$, while solid curve is for $M = 420\text{MeV}$. The dotted curve displays the case of $M = 450\text{MeV}$. The empirical data are taken from Höhler *et al.* [38].

Fig. 2: The neutron electric formfactor as a function of Q^2 : The solid curve corresponds to the constituent quark mass $M=420\text{ MeV}$, while dashed curve draws $M=370\text{ MeV}$. The dotted curve displays the case of $M=450\text{ MeV}$. The empirical data are taken from Platchkov *et al.* [39]. The other four points are results for G_E^n extracted by Woodward *et al.* [40] (open diamond), by Thompson *et al.* [41] (open box), by Eden *et al.* [42] (open circle) and by Meyerhoff *et al.* [43] (open triangle).

Fig. 3: The proton electric formfactor as a function of Q^2 : The solid curve corresponds to the strange quark mass $m_s = 180\text{ MeV}$, while dashed curve draws without m_s . The dotted curve displays the case of the SU(2) model. $M = 420\text{ MeV}$ is chosen for the constituent quark mass. The empirical data are taken from Höhler *et al.* [38].

Fig. 4: The neutron electric formfactor as a function of Q^2 : The solid curve corresponds to the strange quark mass $m_s = 180\text{ MeV}$, while dashed curve draws without m_s . The dotted curve displays the case of the SU(2) model. $M = 420\text{ MeV}$ is chosen for the constituent quark mass. The empirical data (shaded circle) are taken from Platchkov *et al.* [39]. The other four points are results for G_E^n extracted by Woodward *et al.* [40] (open diamond), by Thompson *et al.* [41] (open box), by Eden *et al.* [42] (open circle) and by Meyerhoff *et al.* [43] (open triangle).

Fig. 5: The electric isospin formfactors of the nucleon as a function of Q^2 : The solid curve corresponds to the isoscalar electric formfactor of the nucleon in SU(3), while the dashed curve denotes the isovector one. The dot-dashed curve draws the isoscalar one in

SU(2), whereas the dotted curve stands for the isovector one in SU(2).

Fig. 6: The electric formfactors of the charged SU(3) octet baryons as a function of Q^2 : The solid curve corresponds to the proton electric formfactor. The dashed curve is for Σ^+ . The dash-dotted curve displays that of Σ^- . The dotted curve represents that of Ξ^- . $M = 420$ MeV is chosen for the constituent quark mass.

Fig. 7: The electric formfactors of the neutral SU(3) octet baryons as a function of Q^2 : The solid curve corresponds to the neutron electric formfactor. The dashed curve is for Λ . The dash-dotted curve displays that of Σ^0 . The dotted curve represents that of Ξ^0 . $M = 420$ MeV is chosen for the constituent quark mass.

Fig. 8: The proton magnetic formfactor as a function of Q^2 : The dashed curve corresponds to the constituent quark mass $M = 370$ MeV, while solid curve is for $M = 420$ MeV. The dotted curve displays the case of $M = 450$ MeV. The empirical data are taken from Höhler *et al.* [38]. The numbers are given in units of the Bohr-magneton without any rescaling.

Fig. 9: The neutron magnetic formfactor as a function of Q^2 : The dashed curve corresponds to the constituent quark mass $M = 370$ MeV, while solid curve is for $M = 420$ MeV. The dotted curve displays the case of $M = 450$ MeV. The empirical data represented by black dots are taken from Höhler *et al.* [38] while the data with open triangles are due to the most recent experiment [47]. The numbers are given in units of the Bohr-magneton without any rescaling.

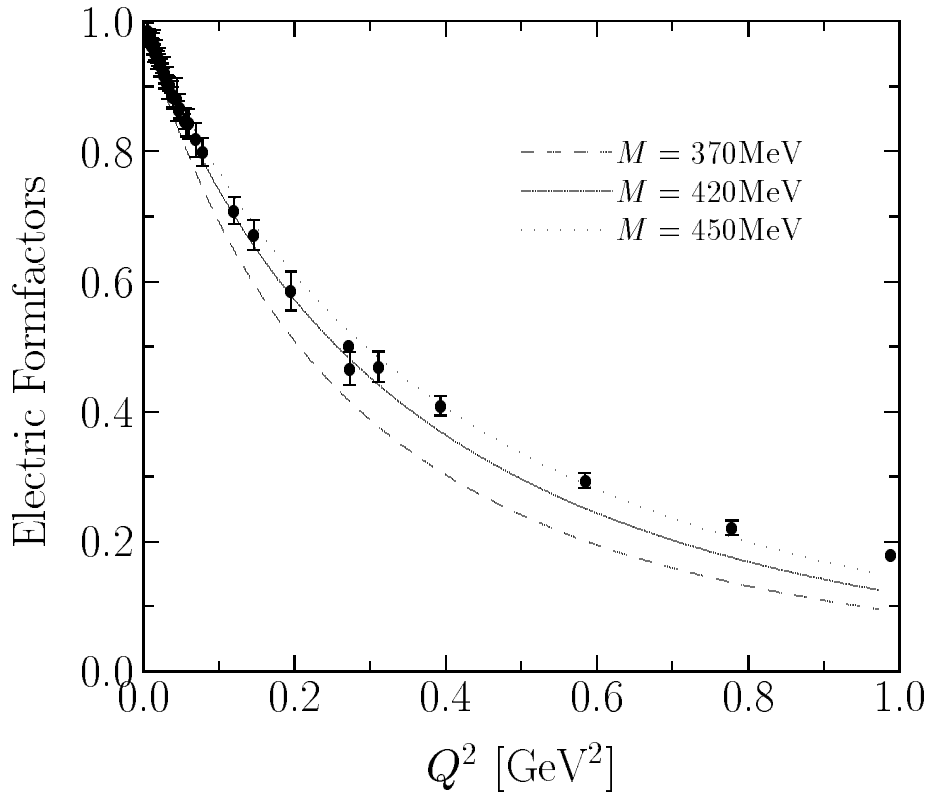
Fig. 10: The proton magnetic formfactor as a function of Q^2 : The solid curve corresponds to the strange quark mass $m_s = 180$ MeV, while dashed curve draws without m_s . The dotted curve displays that of the SU(2) model. $M = 420$ MeV is chosen for the constituent quark mass. The empirical data are taken from Höhler *et al.* [38]. The numbers are given in units of the Bohr-magneton without any rescaling.

Fig. 11: The neutron magnetic formfactor as a function of Q^2 : The solid curve corresponds to the strange quark mass $m_s = 180$ MeV, while dashed curve draws without m_s . The dotted curve displays the case of the SU(2) model. $M = 420$ MeV is chosen for the constituent quark mass. The empirical data represented by black dots are taken from Höhler *et al.* [38] while the data with open triangles are due to the most recent experiment [47]. The numbers are given in units of the Bohr-magneton without any rescaling.

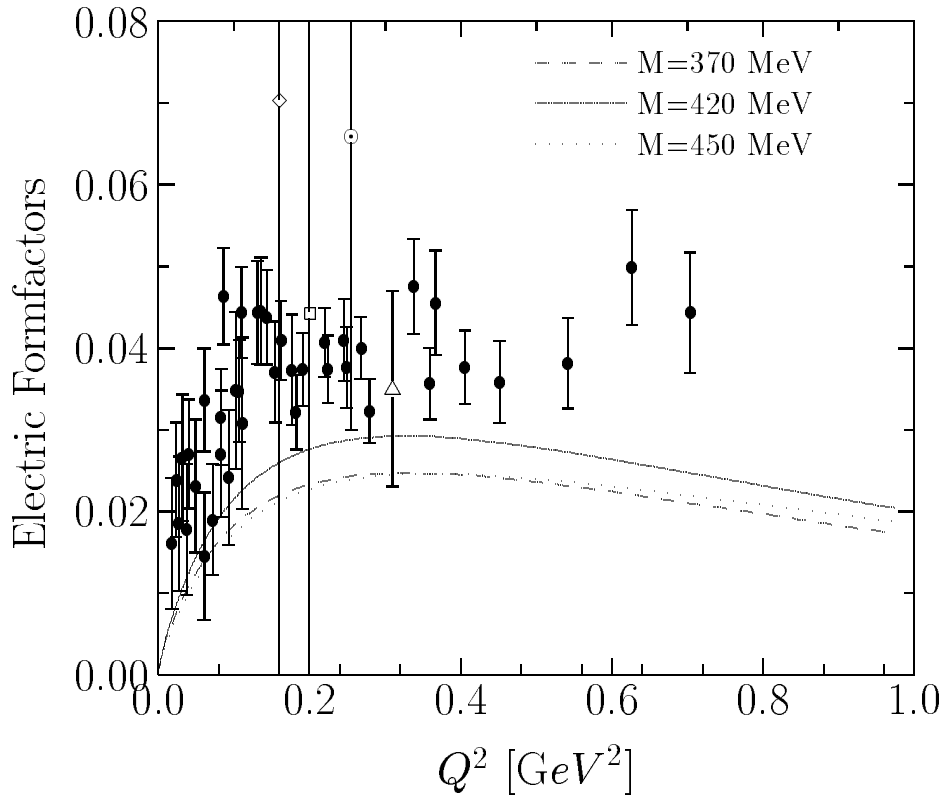
Fig. 12: The magnetic formfactors of the charged SU(3) octet baryons as a function of Q^2 : The solid curve corresponds to the proton magnetic formfactor. The dashed curve is for Σ^+ . The dash-dotted curve displays that of Σ^- . The dotted curve represents that of Ξ^- . The experimental data for the magnetic moments are taken from Ref [46]. $M = 420$ MeV is chosen for the constituent quark mass.

Fig. 13: The magnetic formfactors of the neutral SU(3) octet baryons as a function of Q^2 : The solid curve corresponds to the neutron magnetic formfactor. The dashed curve is for Λ . The dash-dotted curve displays that of Σ^0 . The dotted curve represents that of Ξ^0 . The experimental data for the magnetic moments are taken from Ref. [46]. $M = 420$ MeV is chosen for the constituent quark mass.

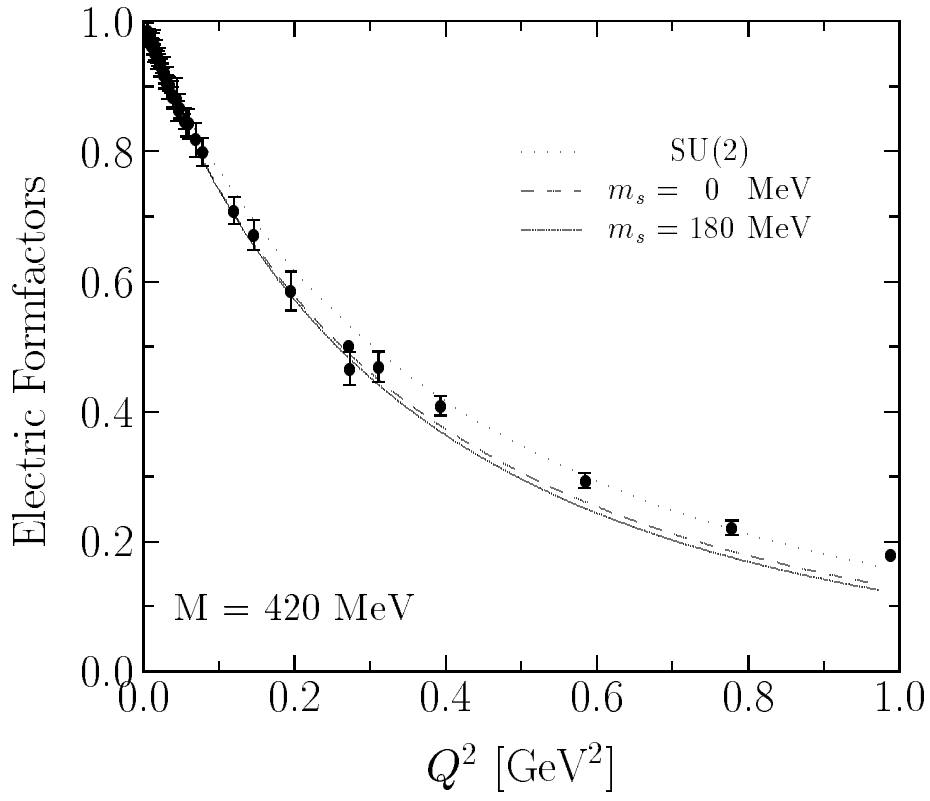
Proton



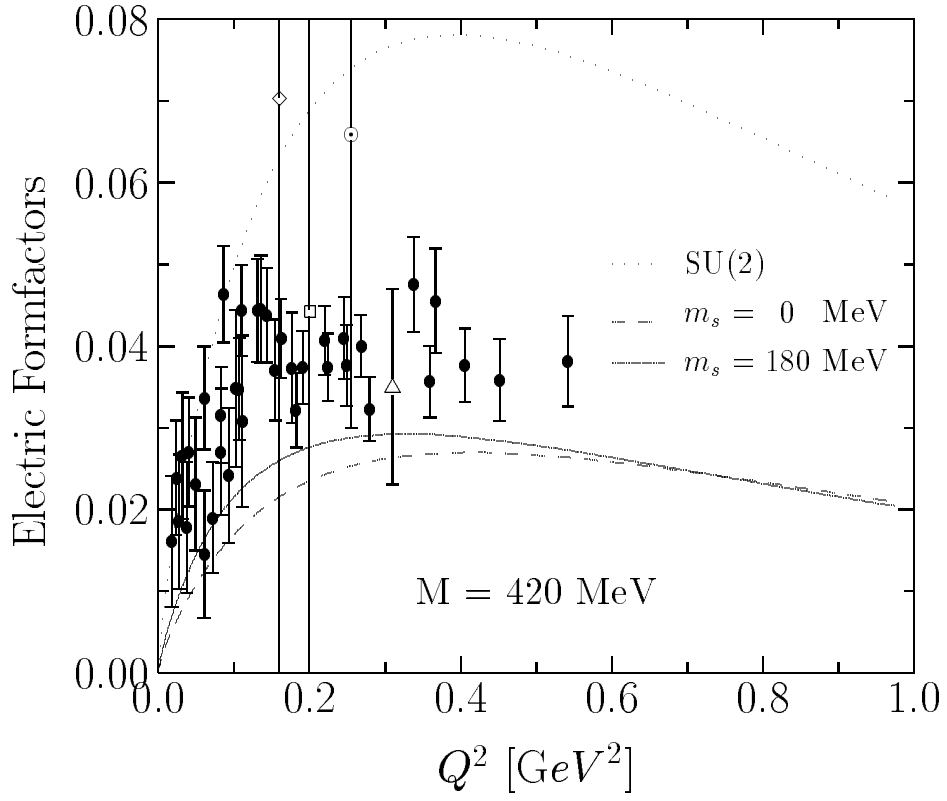
Neutron



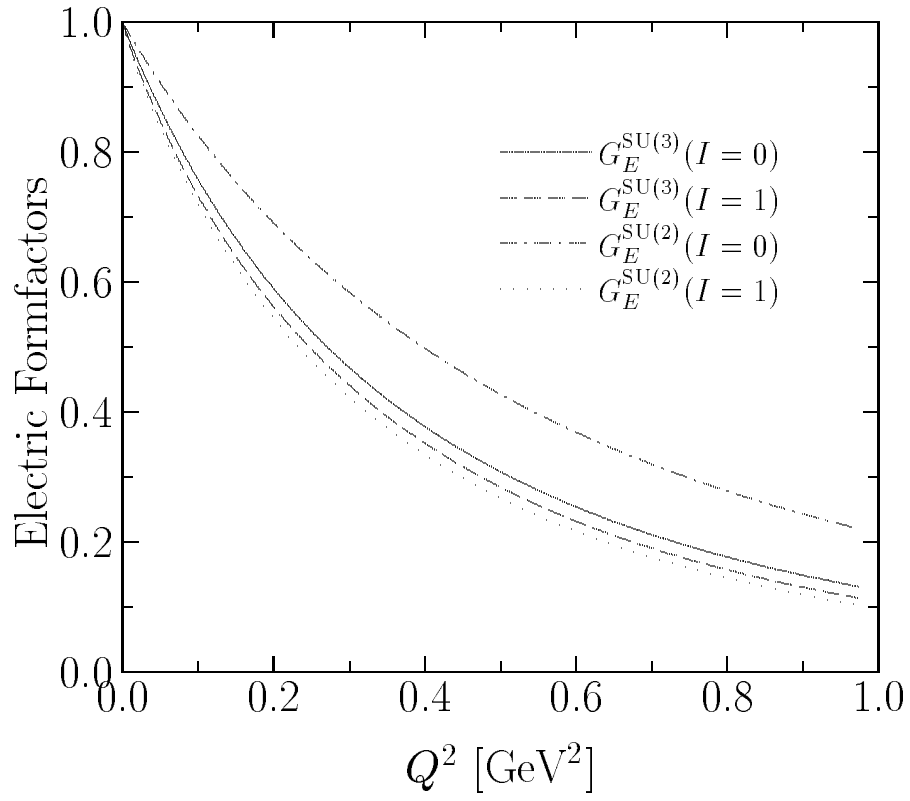
Proton



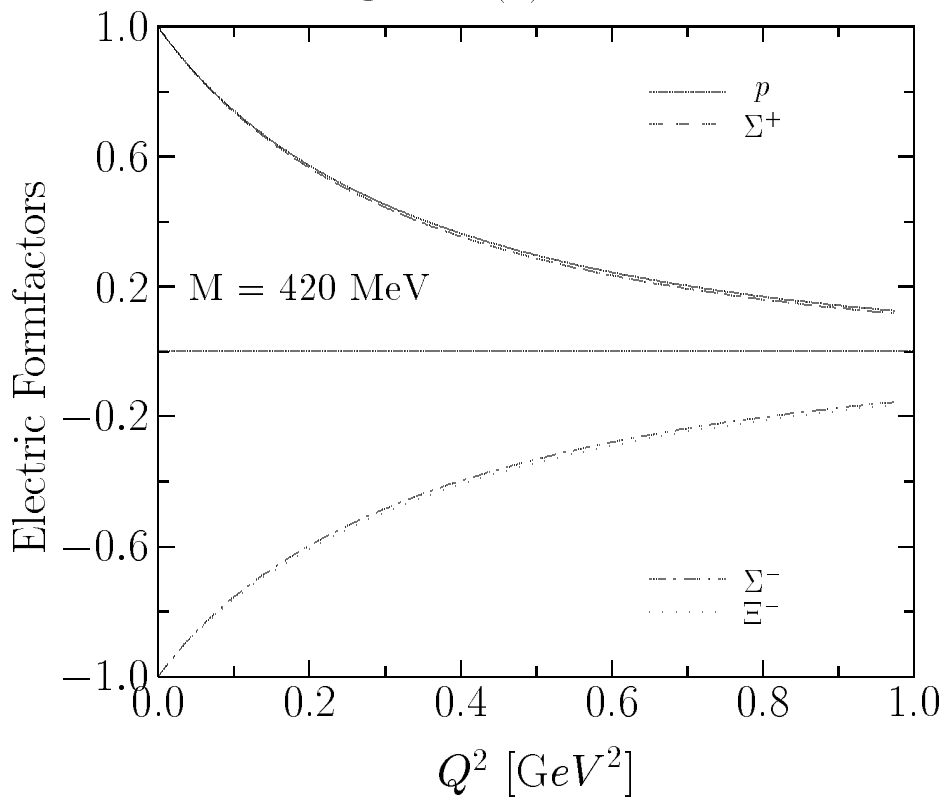
Neutron



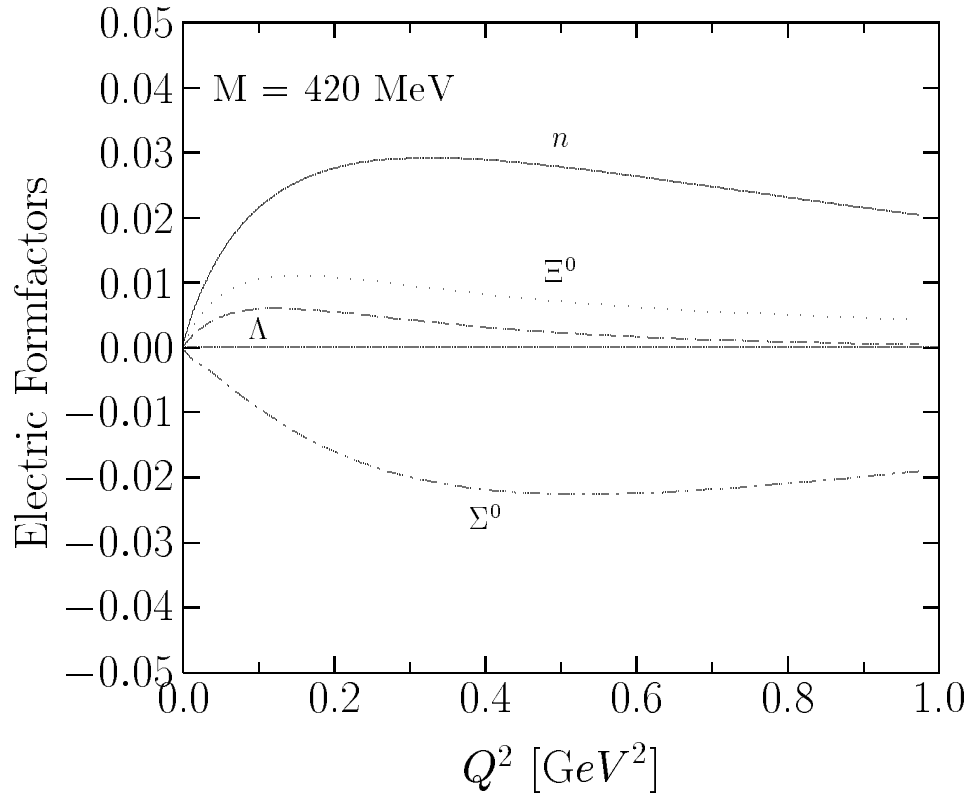
Electric isospin formfactors



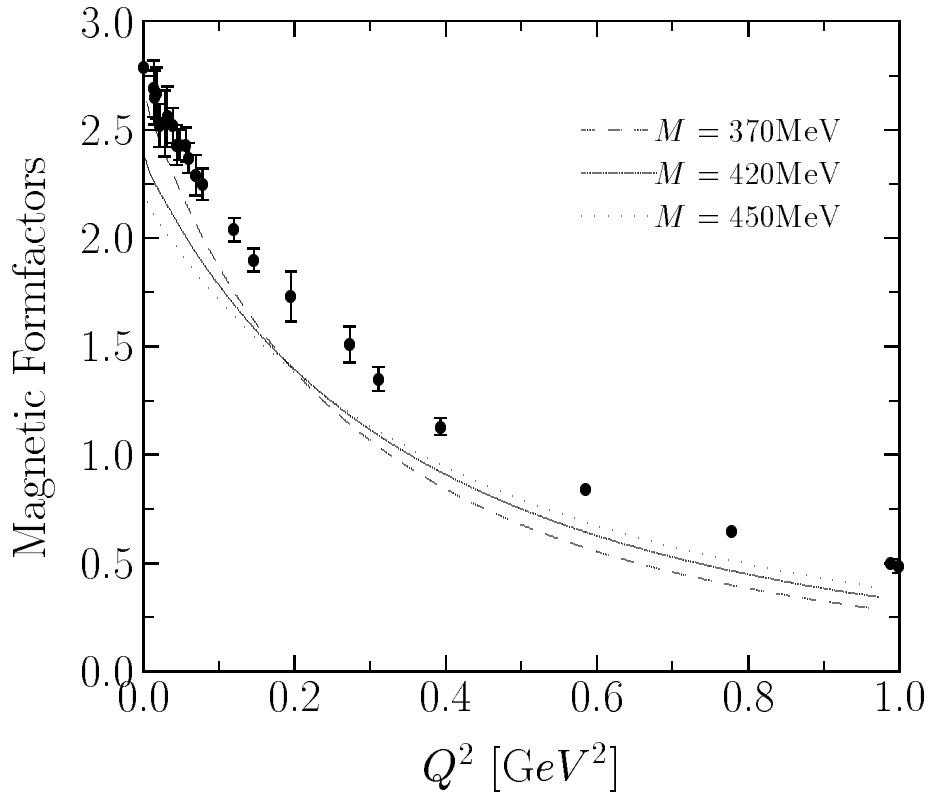
Charged SU(3) octet baryons



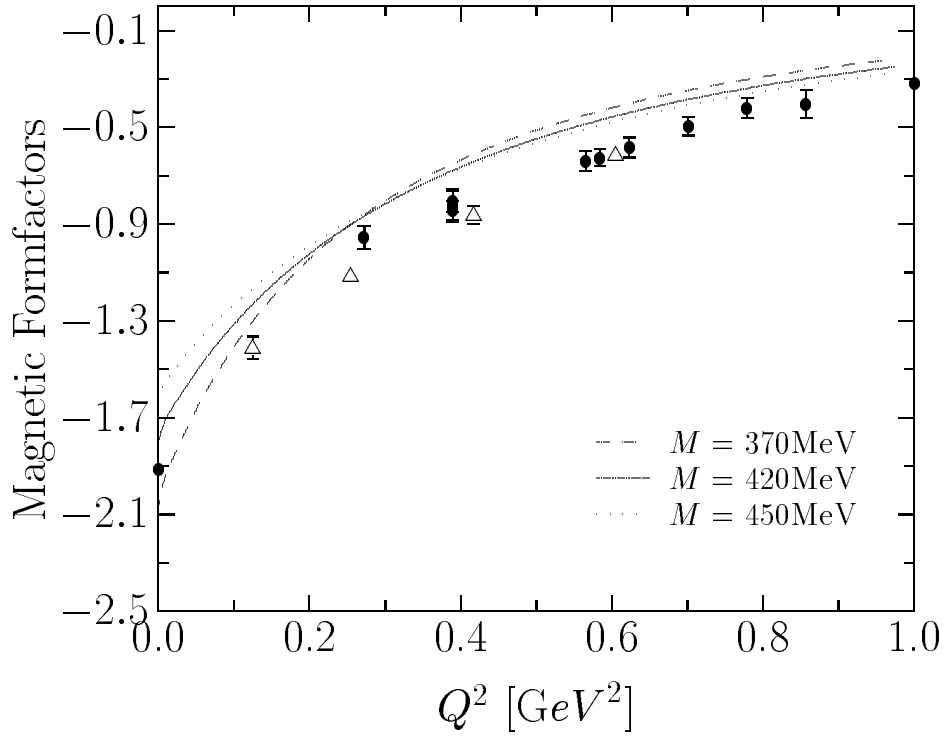
Neutral SU(3) octet baryons



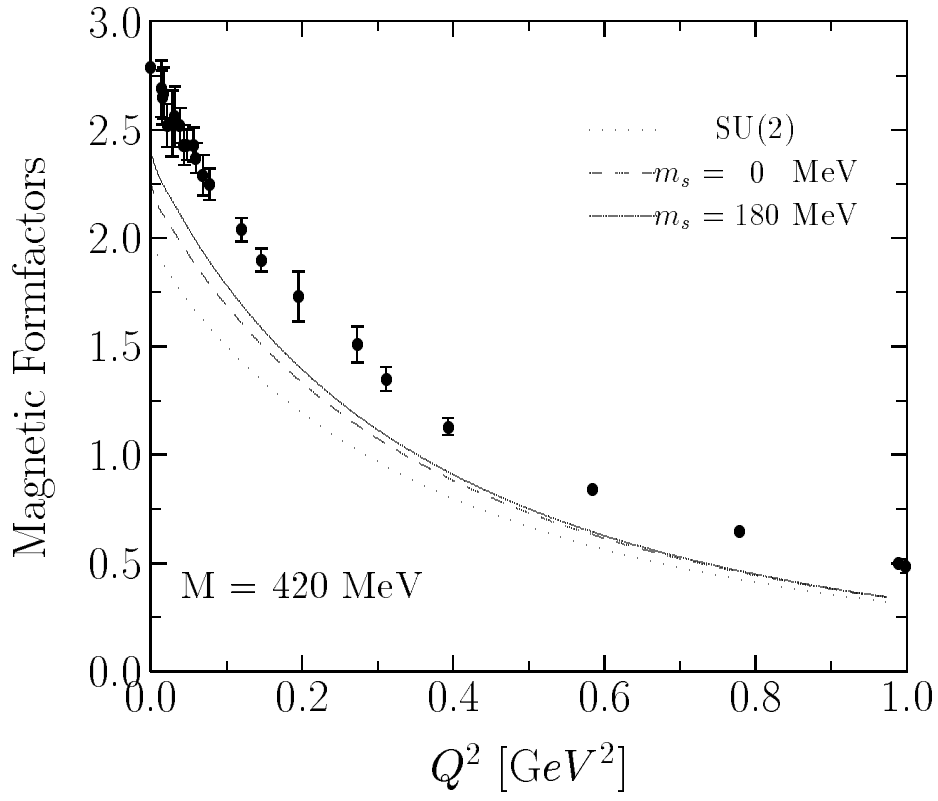
Proton



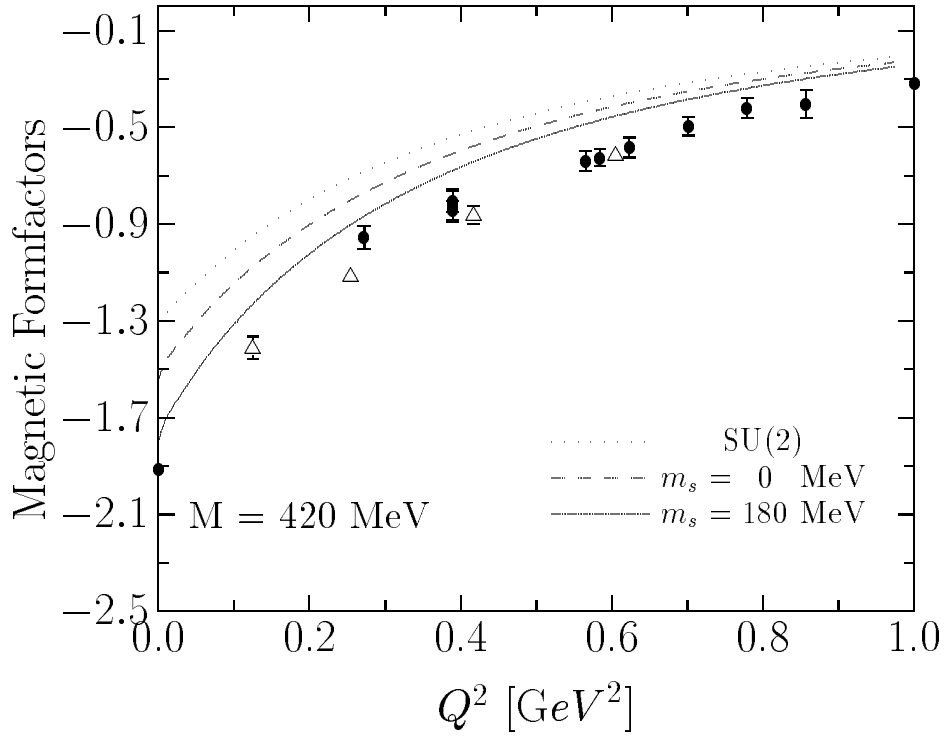
Neutron



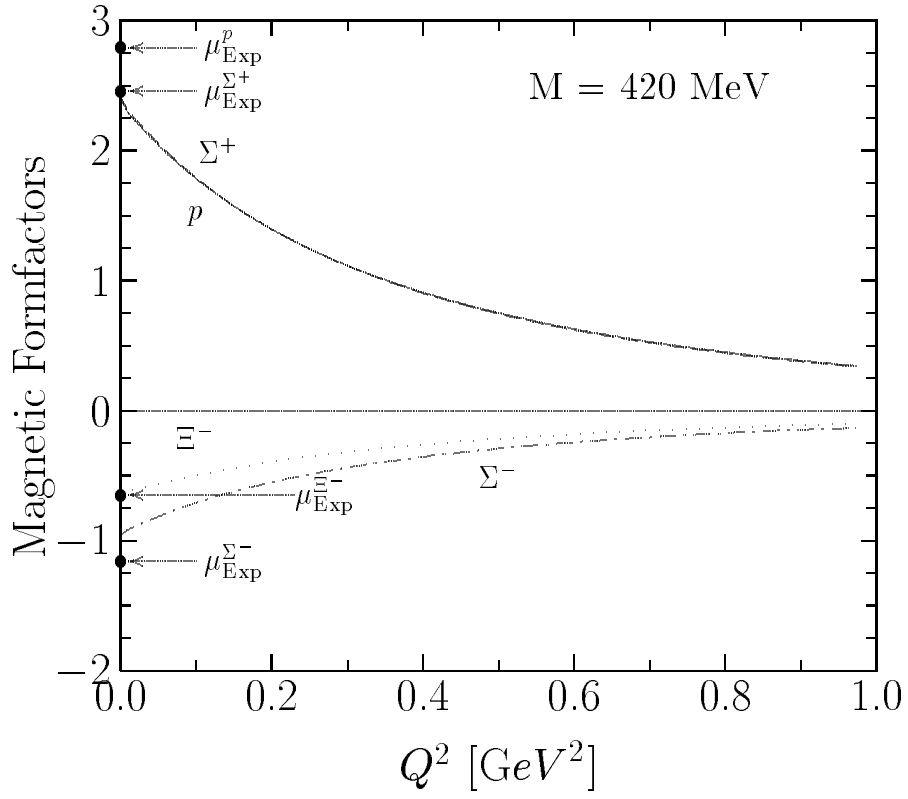
Proton



Neutron



Charged SU(3) octet baryons



Neutral octet Baryons

